Solar Energy 225 (2021) 357–374

Contents lists available at ScienceDirect

Solar Energy

journal homepage: www.elsevier.com/locate/solener

Typical Daily Profiles, a novel approach for photovoltaics performance assessment: Case study on large-scale systems in Chile

Julián Ascencio-Vásquez [a,*], Juan Carlos Osorio-Aravena [b,c], Kristijan Brecl [a], Emilio Muñoz-Cerón [c], Marko Topič [a]

[a] University of Ljubljana, Faculty of Electrical Engineering, Tržaška cesta 25, 1000 Ljubljana, Slovenia
[b] Universidad Austral de Chile, Campus Patagonia s/n, 5950000 Coyhaique, Chile
[c] University of Jaén, Campus Las Lagunillas s/n, 23071 Jaén, Spain

ARTICLE INFO

Keywords:
Photovoltaic
Performance
PV system
Typical Daily Profiles
KPIs

ABSTRACT

A growing photovoltaic industry shows exponential deployment worldwide, and it is expected to largely contribute to the energy transition. Because PV technologies will play a major role in achieving global sustainable development and climate goals, driving more energy-efficient scenarios will require efficient approaches to evaluate systems, especially when dealing with big data of a large region or portfolio. In this work, a novel approach for the PV performance assessment of photovoltaic systems, called "Typical Daily Profiles" (TDP), is presented. This approach is tested on the entire PV fleet operating in Chile from 2014 to 2019. The TDP approach can help to calculate key performance indicators, identify the mounting configuration of PV systems, and to detect major technical issues. A detailed validation carried on the Chilean PV fleet confirms the TDP approach's capabilities to provide accurate PV performance results, neglecting external factors such as failures, grid curtailment, or poor operation activities. Chile was chosen due to the large variety of climate zones in its unique geography, which helps to understand the PV performance under different environmental conditions. Besides, this study reveals the immense potential of PV technologies in Chile compared to mature PV markets worldwide. On an annual basis, their unit capacity factors can reach up to 38%, performance ratios above 90%, and the highest energy yield close to 3350 kWh/kWp. Proving to be an accurate tool, the Typical Daily Profiles approach can be easily applied to other PV portfolios in different regions, and a periodical execution could help to identify and understand long-term performance losses.

1. Introduction

The global photovoltaic (PV) installed capacity shows exponential growth, and it is expected to reach the so-called Terawatt era by 2022–2023 (Haegel et al., 2019). The accelerated PV deployment is evidenced over all climate zones (Solar Power Europe, 2020), even in countries where the PV market is relatively new, and the field experience is scarce. The annual installed PV capacity for 2020 was 140GW, while estimations for 2021 surpass the 160GW globally (Jäger-Waldau, 2021). The competitive numbers achieved by PV are also motivating its use in diverse applications, at different scales and in combination with other renewable and storage technologies (Gaete-Morales et al., 2019; Bustos et al., 2019; Mena et al., 2019; Ramirez Camargo et al., 2019). Because all possible scenarios show an important share of renewables in the global energy matrix, the PV systems will play a crucial role in achieving climate goals by 2050 (Jacobson et al., 2018; Bogdanov et al., 2019). Thus, the effective and continuous performance monitoring and assessment of operating PV systems are crucial to detect any disturbances and maximise the systems' energy yield (Woyte et al., 1013).

The evaluation of the field performance of PV systems typically includes key indicators such as annual energy yield, unit capacity factor (*UCF*), and performance ratio (*PR*) (International Electrotechnical Comission; Ascencio-Vásquez et al., 2019). Accurate results usually require a large amount of time to process field monitoring data (e.g., parsing, cleaning, and filtering) and to gather and interpret historical logbooks (e.g., failure events and technical interventions) (Tjengdrawira et al., 2017; Ascencio-Vásquez and Topič, 2017; Kurtz et al., 2013). An attempt of calculating performance indicators using publicly available data at low resolution (e.g., net generation at annual values) has been published in (Bolinger et al., 2020); the authors have estimated −1.3%/year system-level degradation of a portfolio of 21GW in the United

* Corresponding author.
E-mail address: julian.ascencio.vasquez@gmail.com (J. Ascencio-Vásquez).

https://doi.org/10.1016/j.solener.2021.07.007
Received 11 January 2021; Received in revised form 2 July 2021; Accepted 6 July 2021
Available online 27 July 2021

Nomenclatures

Symbols

G_{PoA}	Global Plane-of-Array irradiance [W/m^2]
H_{ann}	Annual global horizontal irradiation [kWh/m^2]
P_{STC}	DC power of the PV array determined at STC [MW]
P_{net}	Net power [MW]
Y_{net}	Net injected energy yield [kWh/kW$_p$]
Y_r	Reference yield [–]
DHI	Diffuse horizontal irradiance [W/m^2]
DNI	Direct normal irradiance [W/m^2]
GHI	Global horizontal irradiance [W/m^2]
G_{Track}	Global tracking irradiance [W/m^2]
PR_{net}	Net Performance Ratio [–]
UCF_{net}	Net Unit capacity factor [–]
k_c	Clearness index
y_i	Initial year of a time series
y_f	Final year of a time series

Abbreviations

CEN	Coordinador Eléctrico Nacional
CNE	Comisión Nacional de Energía
c-Si	Crystalline Silicon
CSP	Concentrated Solar Power
HSAT	Horizontal Single Axis Tracking
Minenergia	Minister of Energy of Chilean government
PV	Photovoltaics
RE	Renewable energy
SEN	Sistema Eléctrico Nacional
STC	Standard Test Conditions
AVG-TDP	Average Typical Daily Profiles
Y2Y-TDP	Year-to-Year Typical Daily Profiles
TDP	Typical Daily Profiles approach

States, even though the low-resolution data prohibited from properly attributing and allocating the estimated losses to probable causes such module-level degradation, soiling and availability. In (Lindig et al., 2021b), a portfolio of 8367 PV systems with 10-minute time-series of AC power generation was considered for a degradation assessment over large regions. Still, due to outliers and missing data and time-series length criteria, the study was carried out on 51.7% of the available systems. Such examples prove that more and more data is being stored and available for research. However, further algorithms are needed to reduce the percentage of data neglections as well as increasing the number of indicators and features that could be possible to extract from limited PV operational datasets.

The challenge of working with limited PV operational data, together with the need for new models for PV performance assessment, motivated us to develop a new simple and very effective approach called Typical Daily Profiles (TDP). This approach aims to support and accelerate the long-term evaluation of large PV systems portfolios using free-access datasets on a regional or country level.

To prove the great potential and accuracy of the TDP approach, we gathered and processed operational data from the entire PV fleet in Chile. In addition to the convenient sharing data policies followed in this country, Chile shows incredible potential for a large percentage of PV integration to the energy matrix and was already reported as the country with the fourth-highest national PV penetration (i.e., theoretical PV capacity to produce more than 8.5% of their annual electricity demand with PV) (IEA PVPS Task 1, 2020), reaching 2.6 GW of installed PV capacity by March 2020 (Comision Nacional de Energia (CNE) Chile, 2020a). In terms of installed PV capacity per inhabitant, Chile shows 142 W/capita, similar to China (147 W/capita) and France (148 W/capita), above the worldwide number of 83 W/capita, but still far from mature markets as in Australia (637 W/capita), Germany (593 W/capita), Japan (498 W/capita), and Belgium (394 W/capita).

This country counts with unique geography where the latitudes go from −17.51° to −56.02°, with a length of 4337 km, an average width of about 200 km, and the highest elevation on Ojos del Salado at 6893 m above sea level (Moreira-Munoz, 2011). Furthermore, in view of climate zones defined by the Köppen-Geiger-Photovoltaic (KGPV) scheme (Ascencio-Vásquez et al., 2019), the country is divided into Desert with Very High Irradiation zone (24%), Temperate with High and Medium Irradiation zones (20% each), and Polar zone (including high mountains; 25%). This variety of climates makes Chile an exciting country for the research and development of PV technology (Agostini et al., 2016) and PV system evaluations since the different climates can be related to other regions worldwide by using climate classification schemes (Ascencio-Vásquez et al., 2020).

The paper shows the state-of-the-art PV fleet performance assessment, and it described the dataset used concerning the country situation (solar resource and prospects) and important technical aspects and limitations for PV systems operating in Chile. Then, the Typical Daily Profiles (TDP) approach is defined, validated, and applied to different applications using publicly available data in Chile. The validation of the irradiance modelling needed for a traditional performance assessment is carried out on eleven high-quality weather stations. The TDP approach is compared to traditional methods using on-site measurements of four PV systems. Once validated, the algorithm is used over the whole PV fleet in Chile. Finally, we discuss the findings, current limitations, and further recommendations for periodical studies.

2. State-of-the-art on PV fleet performance assessment

The large PV deployment in the last years brings interesting research opportunities to evaluate not only several single PV systems. It brings the chance to evaluate large portfolios aiming to identify geographical patterns and benchmark technologies under different operating environments (Kumar and Kumar, 2017). The state-of-the-art in this shows promising results, but at the same time, several studies reveal limitations due to data quality issues and lack of important information such as soiling, inverter failure, downtime for maintenance and/or similar events.

Early studies in 2012, already handled with a large portfolio of PV systems with limited data. In (Leloux et al., 2012; Leloux et al., 2012), Leloux et al. analysed the performance of 6868 residential PV systems in France, and 993 residential PV systems in Belgium, where the specific yield, performance ratio and performance index have been calculated. Since the datasets included purely residential systems, the presence of curtailment or downtime due to O&M activities are unlikely to be observed in the time series. Thus, the data quality checks are reduced to detect operational unavailability mostly. Later on, in 2015, Leloux et al. analysed over 31,000 residential and commercial PV systems in Europe (over nine different countries) (Leloux et al., 2015). The specific yield for France was 1115 kWh/kWp, for the UK 898 kWh/kWp, for Belgium 908 kWh/kWp, and for Spain 1450 kWh/kWp for fixed-mounting systems and 2127 kWh/kWp for tracking systems. A typical PR of 0.81 is suggested. The detailed information allows to benchmark by technology and year of installation. The PR of new installations show increases of 0.5%/year. As proof of the usability of very large PV portfolio data, in 2020, Leloux et al. developed a robust peer-to-peer (P2P) methodology to detect performance deviations (Leloux et al., 2020) using over 6000 PV systems dataset operating in Europe.

In the United States, the PV Fleet Data Initiative (Deline et al., 2020) aims to collect high-quality PV operational data all over the country. A

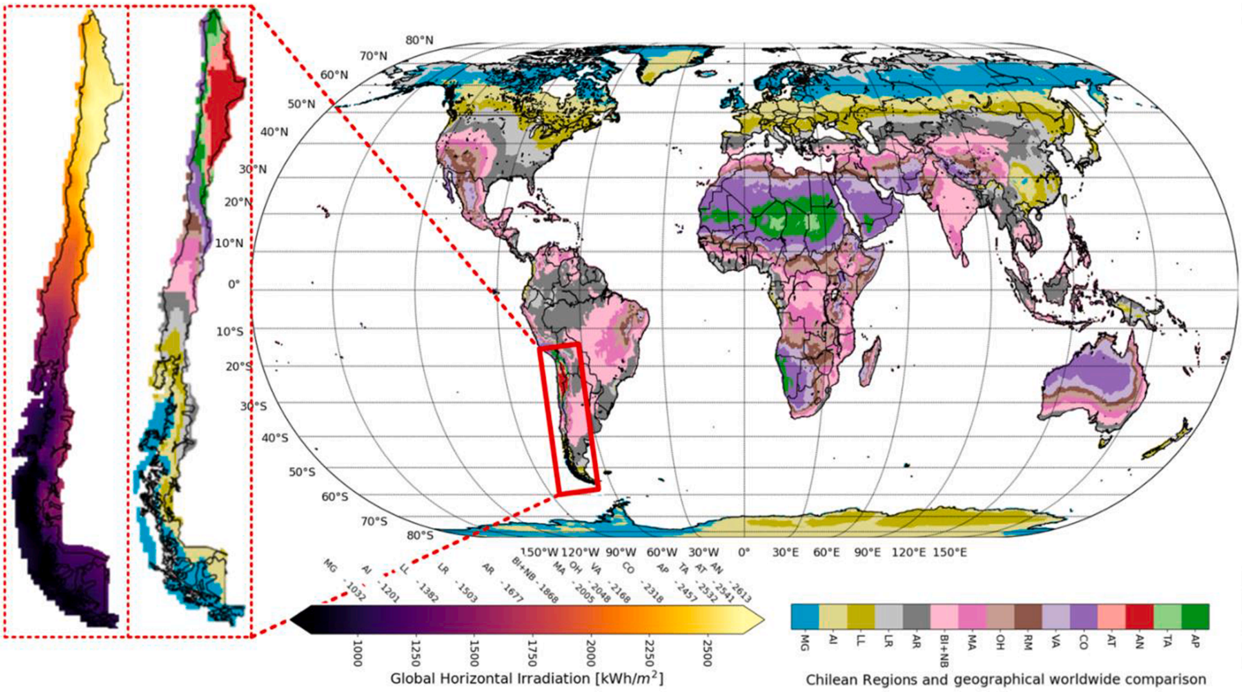

Fig. 1. Worldwide comparison of the solar potential per Chilean region in terms of annual global horizontal irradiation (H_{ann}) in [kWh/m^2]. Name regions defined in ISO 3166-2:CL.

recent report (Deline et al., 2021) shows the analysis on 250PV systems, equivalent to 157 MW on DC side. The monthly Performance Index (PI) is calculated from sub-hourly energy data and satellite-based resource data, together with the identification of first-year start-up issues, snowfall, and inverter downtime. The average monthly PI is reported to be 0.994. Inverter availability contributes in the first six months of operation with availability losses closer to 8%, and on average with a system energy loss of 2.3%. In winter, the performance drops 5% to 10% compared to winter likely due to snowfall.

A similar initiative is being carried out in the frame of the European funded COST Action PEARL-PV (Reinders et al., 2018). A portfolio of 8367 PV systems with a 10-minute time-series of AC power generation has been processed for performance and degradation studies (Lindig et al., 2021b). Considering PV systems with at least one year of data, the average annual yield is 954.9 kWh/kWp and the average performance ratio 76.7%. For degradation indicators, over 90% of the PV systems were excluded due to the strict data filtering process (methodologies reported in (Lindig et al., 2021a), where data is categorized as an outlier or simply having an insufficient length. As a result, the mean Performance Loss Rate (PLR) ranges between −0.74 and −0.75%/year, while the median between −0.36%/year and −0.67%/year depending on the statistical approach chosen.

In (Bolinger et al., 2020), 411 utility-scale PV systems operating in the United States (summing up to 21.1 GW in DC power) have been analysed. The article reports an average system-level degradation rate of −1.3%/year (±0.2%), which is higher than commonly expected −0.5%/year. The authors claim that the excessive degradation rate obtained is impacted by not only module degradation but also system degradation, system availability, component failures and events. Unfortunately, such information is not available when using public sources and low-resolution data.

A fleet of 57 PV plants operating in India and Southeast Asia has been analysed (Nobre et al., 2019). With more background information about the operation of the PV plants, the authors reached to label the results; for example, low PR due to heavy soiling has been detected in the PV systems in the North of India, and low PR in Cambodia and the Philippines due to low load or curtailment. Interestingly, the system-degradation rates mentioned above for the US (average −1.3%/year) is comparable to the average system-level degradation rate in India equal to −1.2% (based on 12 PV plants), while for Cambodia is −1.1% (based on 4 PV plants), in the Philippines is −0.9%/year (based on 4 PV plants), and in Singapore is −0.8%/year (based on 4 PV plants).

When analysing one or a few systems, the PV performance assessment is typically carried out using high-quality weather time-series as input data (e.g., on-site sensors for irradiance, temperature and wind speed) and energy production as output (Ascencio-Vásquez et al., 2020). In addition, knowledge about the mounting structure, technologies and equipment installed, operation and maintenance (O&M) logbooks, and failure reports can also largely help understand the PV system's historical operation. However, as observed in previous publications and through this work, when analysing a whole fleet of PV systems, the complementary data is usually missing or limited.

This paper proposes a new approach to analyse large utility-scale PV fleets using limited data publicly given for transmission system operators. Compared with residential and commercial systems, the utility-scale systems could present more performance deviations and anomalies, making it a more challenging task for executing the performance assessments using limited data. The Typical Daily Profiles (TDP) approach explained further try to help to get reliable performance indicators. Also, the algorithm aims to reduce the percentage of data neglections and increase the number of indicators and features that could be possible to extract from limited PV operational datasets.

3. The PV industry in Chile

To better understand the dataset used in this paper, the solar resource in Chile is evaluated in comparison with other locations worldwide. Then, specific technical aspects in the operation of PV systems in Chile are given. Finally, the dataset used is described.

3.1. Regional solar resource and worldwide comparison

Chile has been identified as the country with the highest solar irradiation worldwide in the Atacama Desert (Hirschmann, 1973; Rondanelli et al., 2015), yet the great potential is also perceived in other

Table 1
Main failures of eight large scale PV systems in Chile (Source: Encare, Energia 360, 2017).

Main Section		Specific components/failures	
Conversion Units	49%	Inverter – Control	36%
		Inverter – Force	21%
		Inverter – Temperature	16%
		Inverter – Force components	8%
		Transformer - Mechanical faults	7%
		Transformer – Temperature	6%
		Others	6%
PV modules	27%	Cracks	96%
		Hotspots	3%
		Connectors	1%
Medium Voltage installations	9%	Connections - Power Mast	82%
		Connections - Terminals	13%
		Mechanical Faults	5%
Low Voltage installations	7%	Fuses	97%
		Connectors	3%
Tracking systems	5%	Control Faults	38%
		Mechanical Faults	44%
		Electrical Faults	18%
Communication	2%	Hardware	77%
		Main link connection	23%

regions of the country.

In Fig. 1, the solar potential of each region is compared to the locations around the World. The comparison is made on annual global horizontal irradiation (H_{ann}) derived from the ERA5 dataset (Copernicus Climate Change Service (C3S), 2017). The colour of a location in the global map can be directly compared with a Chilean region's potential. The irradiation ranges of each region are presented in Appendix A. The region abbreviations are defined from the standard ISO 3166-2:CL (International Organization for Standardization, 2018). This graphical representation helps to understand the variety of Chile, where almost any location in the World can be related to a Chilean region in terms of solar irradiation.

For example, the solar irradiation in the region of Aysén (abbreviated as AI, with H_{ann} equal to 1201 kWh/m^2) is comparable to Germany, while the region Los Lagos (LL, 1382 kWh/m^2) can be related to the North of Italy or South of France; countries where the PV market is already in a mature stage, and the Levelized-Cost-of-Electricity (LCOE) from PV systems is reported cheaper than average spot market electricity all over Europe (Vartiainen et al., 2019).

The large potential for solar technologies is aligned with the predictions of the future Chilean energy system (Haas et al., 2018b; Haas et al., 2019; Osorio Aravena et al., 2020). Their findings show that 100% renewable-based power generation in Chile will be technically feasible and economically viable by 2050, and according to (Osorio Aravena et al., 2020), solar PV could supply at least 39% of the electricity needs with an installed PV capacity of 43.6 GW.

Renewable electricity is pivotal for the sustainable energy transition in Chile. In particular, solar PV technology, based on its more than 1200 GW of available potential (Ministerio de Energia, Gobierno de Chile, 2014), will be the key to supporting the deployment of electromobility (Girard et al., 2019) and the development of the green hydrogen industry in the country (Armijo and Philibert, 2020). Besides, solar PV systems will play a crucial role in achieving carbon neutrality (Palma Behnke et al., 2019). They could also be the primary driver for the clean production of some feedstocks in Chile, such as copper and lithium, in order to contribute to the global free-carbon economy (Haas et al., 2020).

3.2. Technical aspects of PV systems in Chile

The total installed large-scale PV capacity is connected to the National Electric System (or SEN, Sistema Eléctrico Nacional), growing exponentially from 2012 (Haas et al., 2018a), reaching 2648 MW of installed PV capacity and over 168 large-scale PV systems by the end of 2019.

The predominant technology employed in the PV market in Chile is based on crystalline silicon (c-Si) solar cells (Zurita et al., 2018). In terms of mounting structures, the horizontal single-axis tracking (HSAT) systems predominate the market, followed by the traditional tilted-fixed mounting PV systems. The HSAT mounting structure is preferred due to the advantages in sunny locations, where energy production is maximised and angular reflection losses minimised (Afanasyeva et al., 2018). More recent developments are also presented in the Chilean PV market: three PV systems use bifacial PV modules (La Silla – 1.89 MW, Hormiga Solar – 2.5 MW, and Cordillerilla Solar – 1.33 MW) (Stefano et al., 2017; Liang et al., 2019); and test facilities in the Atacama Desert to support the design of new products adapted for high irradiation and desert conditions (ATAMOSTEC, 2020).

As drawbacks, limitations of the PV deployment in the country have been mainly caused by technical barriers at the electrical grid level, where disconnections due to voltage and security have been carried out. Several large-scale PV systems in the north of the country have been affected by curtailment since 2015 (PV Tech.org, 2016; BloomberfNEF, 2019). The curtailment losses decreased notably in 2019 and the beginning of 2020, but by September, they raised again to 4.3% (for solar and wind together) (Antuko, 2020; Revista Electricidad, 2020). The upgrading plans for transmission lines consider a DC-link of 500 kV between the north and the central region (Santiago) to improve energy transfer. However, estimations show curtailment of over 11% in solar PV by 2025 and a steady decrease to around 5% by 2043 (Coordinador Electrico Nacional, 2021).

Also, energy losses due to soiling may be high in the northern region of the country. The highest daily soiling rates have been estimated to be located in Arica (above 0.4%/day) and tend to observe higher rates in zones closer to the Pacific ocean based on desert dust (Cordero et al., 2018). In Santiago, Urrejola et al. have measured average soiling rates between 0.13 and 0.43%/day in different seasons driven by urban pollution (Urrejola et al., 2016). Considering a cleaning cost between 5 and 10 USD/kWp, the PV modules should be cleaned every 45 to 75 days in Arica and Santiago, while in zones with a soiling rate between 0.2 and 0.4%/day, the cleaning should be executed every 3 to 4 months (Cordero et al., 2018; Urrejola et al., 2016).

Common failures of eight utility-scale PV systems in Chile have already been reported (Encare, Energia 360, 2017). As presented in Table 1, the main components prone to failure are the conversion units (inverters and transformers), followed by failures on the PV modules (27%), Medium and Low Voltage installations (16%), tracking systems (5%) and the communication (2%). Those values are reported in terms of frequency of occurrence. However, failure severities are not reported in terms of energy losses. For instance, central inverters failures can reflect large energy losses and even the shutdown of the whole PV system. In the case of the PV modules, the most reported failures are the cracks produced by either transportation, vandalism, or mechanical loads such as gusts of winds. In any case, the understanding of the solar PV systems performance in Chile is only getting started, and it requires more research and analysis for performance degradation monitoring and failure maintenance.

3.3. Data availability for this study

3.3.1. Large-scale PV power plant data in Chile

The power generation fed to the electrical grid is available online in the "Energía Abierta" platform developed by the "Comisión Nacional de Energía" (CNE) of the Ministry of Energy of Chilean government (Minenergia) (Comision Nacional de Energia (CNE) Chile, 2020b). Time series of PV systems are retrieved on an hourly basis from 1st January 2014 to the 31st December 2019. In this platform, geographical coordinates (Latitude and Longitude) and the limit of the AC power injection, hereby named as "net power" (P_{net}), are also available. The quality of the net power time-series available can be considered as high-quality since it is the one used for transmission system coordination, invoicing, reporting, and planning nationally. The details of each PV power plant, named randomly as "Chile_x" where × ranges from 1 to 168, are presented in Appendix B. For a few systems, the mounting

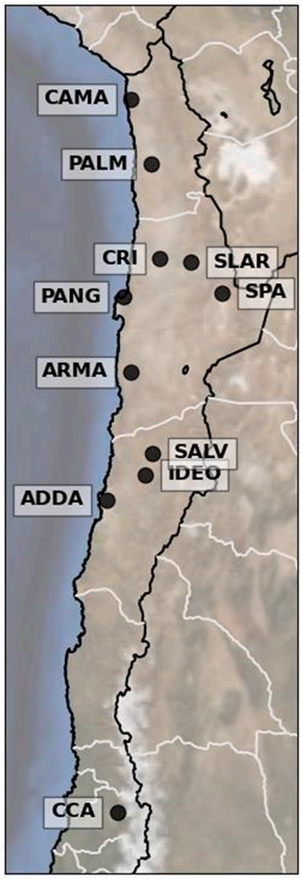

Fig. 2. Locations of 11 weather stations.

Table 2
Geographical coordinates and altitude of available weather stations.

Station	Lat. [°]	Long. [°]	Alt. [m]
ADDA	−27.26	−70.78	210
ARMA	−24.63	−70.24	2581
CAMA	−18.86	−70.22	795
CCA	−33.4	−70.54	850
CRU	−22.27	−69.57	1176
IDEO	−26.75	−69.91	1541
PALM	−20.26	−69.78	1024
PANG	−23.07	−70.39	10
SALV	−26.31	−69.75	1617
SLAR	−22.34	−68.88	2047
SPA	−22.98	−68.16	2390

conditions were identified by observing the data and confirmed with data taken from (Zurita et al., 2018). Most of the PV systems are installed either in fixed-tilted mounting, in the paper denoted as "Fixed", or in HSAT structures, denoted as "Tracking".

3.3.2. Irradiance data

Climate reanalysis datasets have proved to be a valuable option if no local weather data is available (Camargo and Schmidt, 2020). We use the "ERA5" dataset created by the European Centre for Medium-Range Weather Forecasts (ECMWF), which includes global gridded data with a spatial resolution of 31 km and temporal resolution on an hourly basis (Copernicus Climate Change Service (C3S), 2017). The global horizontal irradiance (*GHI*) for the location of each PV system have been extracted.

Measured irradiance data is obtained through the "Explorador Solar" project developed by the Minenergia, which provides cost-free solar irradiance data for eleven locations (Ministerio de Energia, Gobierno de Chile, 2014) (see Fig. 2 and Table 2). This data is collected in 10-minutes resolution with certified measurement devices Kipp&Zonen CMP10/CMP11 (Girard et al., 2019). At all weather stations, the solar irradiance is not only measured at the horizontal plane but also in the East-West Horizontal Single Axis Tracking (HSAT) plane. Periodical maintenance, cleaning and calibration activities have been reported (e.g., monthly for station CRU, and quarterly for station CCA).

4. The TDP approach – A new approach for a big picture analysis

The analysis or extraction of daily profiles in the energy sector is a very convenient approach used to understand electrical demand and consumption behaviour at different scales (region, country, etc.) (Boait et al., 2015; Csoknyai et al., 2019; Valdes et al., 2021), or used in some forecasting techniques where expected profiles could be retrieved from time-series profiles (Prina et al., 2020). However, daily profiles have not been used so far to evaluate the performance of operating PV systems. The Typical Daily Profiles (TDP) aims to be an effective technique to help in the extraction of performance indicators of large utility-scale PV fleet, even more, when limited data is available.

Hence, this work aims to define a new methodology to infer missing information and lead to a PV performance assessment of a large number of PV systems under normal operational conditions, neglecting local and temporal issues such as curtailments, conversion unit failures or missing data. This feature makes the TDP approach a novel method for the PV community.

4.1. Definition of the Typical Daily Profiles (TDP) approach

A lack of relevant information about the PV systems motivated us to design a new method to achieve a PV performance assessment, where undocumented temporal events (e.g., curtailment periods, failures, O&M activities) need to be neglected as much as possible to focus the evaluation to pure components' performance, and to evaluate the long-term behaviour of the PV system. Thus, the Typical Daily Profiles (TDP) approach has been developed to achieve the mentioned goals, basing the formulation on temporal periodicity principles as stated below:

- The time series of solar irradiation and PV power production have a strong periodicity.
- The daily power profile of PV systems shows a rise in the morning, one or two peaks during the day, a decrease in the afternoon, and of course, zero during nights.
- This profile is repeated daily throughout the year, adding two more factors: seasonality and cloudiness.
- The seasonality is location-specific and generally observed in the quasi-sinusoidal periodicity with higher values during summertime and lower values during wintertime.
- The cloudiness is harder to identify, but still, seasonal patterns can be observed: the clearness index (k_c), defined as the ratio of the real and clear-sky irradiance, is lower in winter and higher in summer, and tropical cyclone and storm seasons usually occur in specific periods of a year.

The periodical factors can be simplified by calculating the Typical Daily Profiles (TDP). The TDP gives the hourly profile of a typical day per month of solar irradiance or output power production based on data from a pyranometer or PV system, respectively. In comparison with the Typical Meteorological Year (TMY) calculations (Cebecauer and Suri, 2015; Huld et al., 2018), which represents the climate of a specific location over the 8760 h of the year using ten or more years of climate data, the TDP gives a simplified representation of 24 h-data per month requiring less input data.

4.2. Calculation of Typical Daily Profiles (TDP)

The TDP approach can be defined as a simplified model of time series

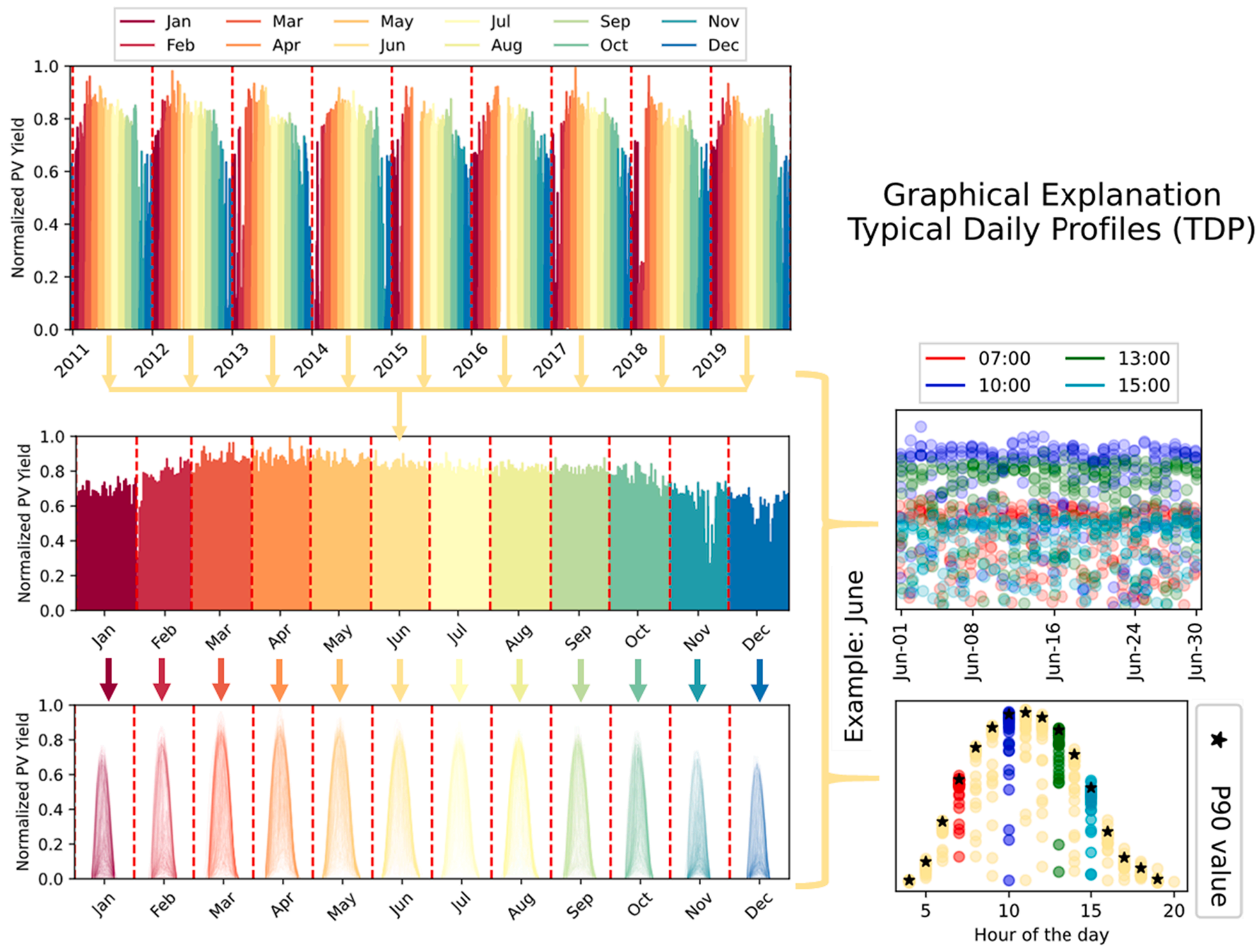

Fig. 3. Practical example of the AVG-TDP approach applied to nine years of measured PV energy yield.

(e.g., irradiance or PV power production). The methodology slightly differ for two different types of clustering: (a) "Average TDP" (or "AVG-TDP") is generated by clustering the time-series by month and hours from the whole dataset (one or more years of data); (b) "Year-to-Year TDP" (or "Y2Y-TDP") is generated by clustering by years, months and hours (from year to year)For each cluster, a mathematical operation is used to extract the most optimistic scenario (e.g., clear-sky conditions equivalent to the percentile 90th value for each group).

An example of the procedure to extract the AVG-TDP is illustrated in Fig. 3, where nine years of operational PV energy yield are processed. The time series is resampled to hourly temporal resolution, then grouped by months and hours, and finally, the percentile 90th is extracted per each hour of the month (see the example for June). The result shows that using the 90th percentile as a mathematical operation can provide an optimistic scenario of PV energy production, as it would be expected for clear sky conditions.

4.3. Application of the TDP approach on large-scale PV systems

Following the practical example of Fig. 3, we apply the methodology to large-scale PV systems. To ensure a performance assessment under similar operating conditions, the P90 scenario seems to neglect underperformances due to O&M activities, weather fluctuations, and failures. Thus, the P90 is chosen as the mathematical operation in the rest of the paper. This choice is confirmed by observing the TDPs from real monitored power output of the PV system CHILE_139 (103.02 MW/Tracking, located in Colina, Chile at 700 m altitude, see Fig. 4.a and 4.b). Fig. 4.c shows two examples of the distribution of power output, where the peaks represent the most common operating conditions during summer and winter at solar noon.

The differences between the AVG-TDP and the Y2Y-TDP are illustrated in this case study. The AVG-TDP using percentiles 50th and 90th are illustrated in Fig. 4.d, reflecting the average and optimistic behaviour during a specific month. The Y2Y-TDP is illustrated in Fig. 4.e, where is evident the underperformance during the first months of operation, as well as a reduction of the power output during the wintertime due to more cloudy days and most probably shading caused by near mountains. The low performance is only observed in the Y2Y-TDP, where the analysis is carried out for a single year, while the AVG-TDP does not show such losses and provide typical production profiles at expected operating conditions.

In further stages, the calculation of TDPs for all PV systems is carried after applying simple preliminary filtering stages: (1) the months containing less than 15 days of useful data are removed; (2) the days with the same generation along the daytime (i.e., square shape generation) are removed; and, (3) the normalised energy yields higher than 1.2 are removed.

4.4. Identification of mounting structure type of PV systems based on P90 AVG-TDP

The mounting structure type can be recognised from the P90 AVG-TDP of PV power production calculated during summertime. Fig. 5 illustrates examples of normalised production profiles (power output divided by net power, P_{net}) for selected PV systems and normalised irradiance (irradiance divided by 1000 W/m^2) for selected pyranometers. The mounting conditions for selected systems are already known (Zurita et al., 2018).

For fixed systems (Fig. 5.a), profiles for horizontal and tilted mounting follow the same pattern for irradiance measurements (in Atacama Desert at CRI station) and PV power production (CHILE_7,

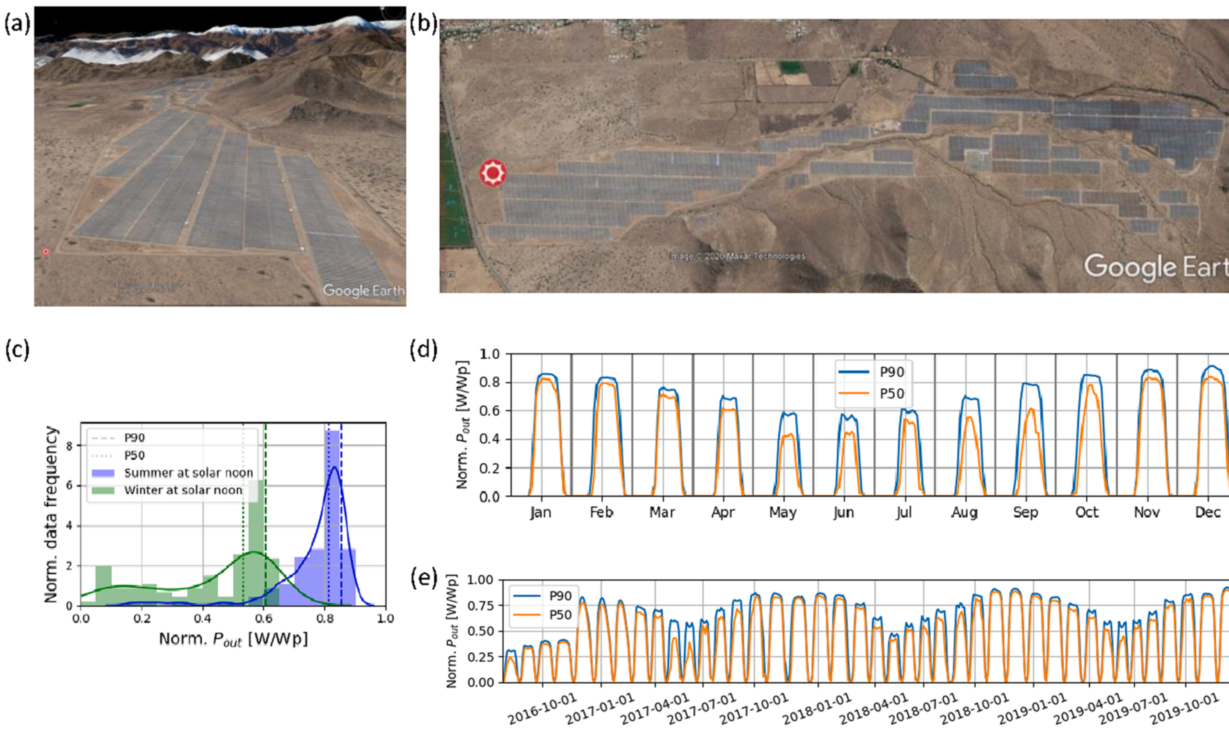

Fig. 4. TDP calculations in CHILE_139, 103.02 MW/Tracking located in Colina, Chile. (a) Angle viewpoint where high mountains are observed close to the PV system (source: Google Earth). (b) Top-viewpoint of the PV system (source: Google Earth). (c) Distributions of power output during summer and winter at solar noon. (d) Average Typical Daily Profile using percentiles 50th and 90th. (e) Year-to-Year Typical Daily Profile using percentiles 50th and 90th.

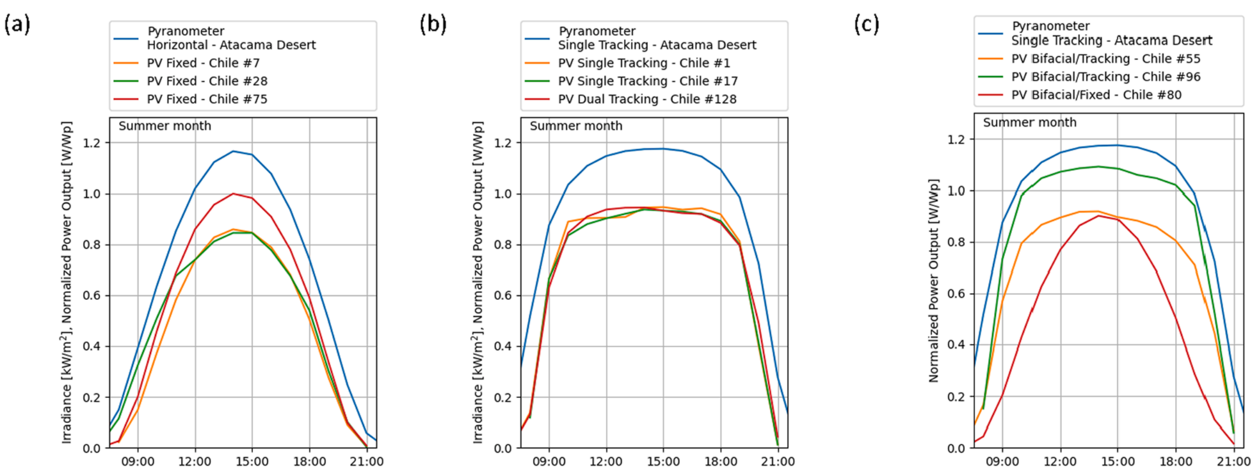

Fig. 5. Typical Daily Profiles using the 90th percentile for (a) Fixed structures, (b) Tracking structures, and (c) Bifacial PV technologies.

CHILE_28, and CHILE_75 presented).

Daily profiles of both single and dual tracking systems show a quasi-squared shape (CHILE_1, CHILE_17, CHILE_26, and CHILE_128 in Fig. 5.b). No significant differences can be observed in profiles of monofacial and bifacial PV technologies (Fig. 5.c).

Due to the lack of information about the mounting structure type in most of the PV systems, a new method based on the P90 AVG-TDP has been developed to differentiate between fixed and tracking systems.

In the model, two statistical indicators are needed: the *kurtosis* and the *skewness* calculated from the average P90 AVG-TDPs. The *kurtosis* indicates whether the distribution of points is heavy or light-tailed compared to a normal distribution. The *skewness* indicates how symmetrical the distribution of points is. More details about the formulation of kurtosis and skewness are given in (National Institute of Standards and Technology). Those two statistical indicators help to differentiate between fixed and tracking PV systems due to their differences in the daily distribution of PV power output.

To create the model, we used 72 systems for training by observing the data and cross-validating with the information given in (Zurita et al., 2018). By plotting *kurtosis* vs *skewness* extracted from each system with known mounting information (see Fig. 6.a), two trends can be observed: one group for "fixed" mounted PV systems and a second group for "tracking" mounted PV systems. Those two groups are modelled by fitting exponential equations named "Fixed" and "Tracking", which are shown inside the plots. The accuracy of this method on the training set gives 30 out of 30 correct labels for fixed PV systems, while for tracking systems, the model helps to identify correctly 40 out of 42 systems. This fact suggests the high reliability of the method.

To fulfil the mounting identification of the remaining 96 PV systems, the pair "kurtosis, skewness" is overlapped to both exponential lines. The shorter distances against both lines are calculated, and the minimal distance identifies the label (see Fig. 6.b).

The identification over the whole fleet of PV systems classifies 59 Fixed and 109 Tracking large-scale PV systems in Chile by the end of

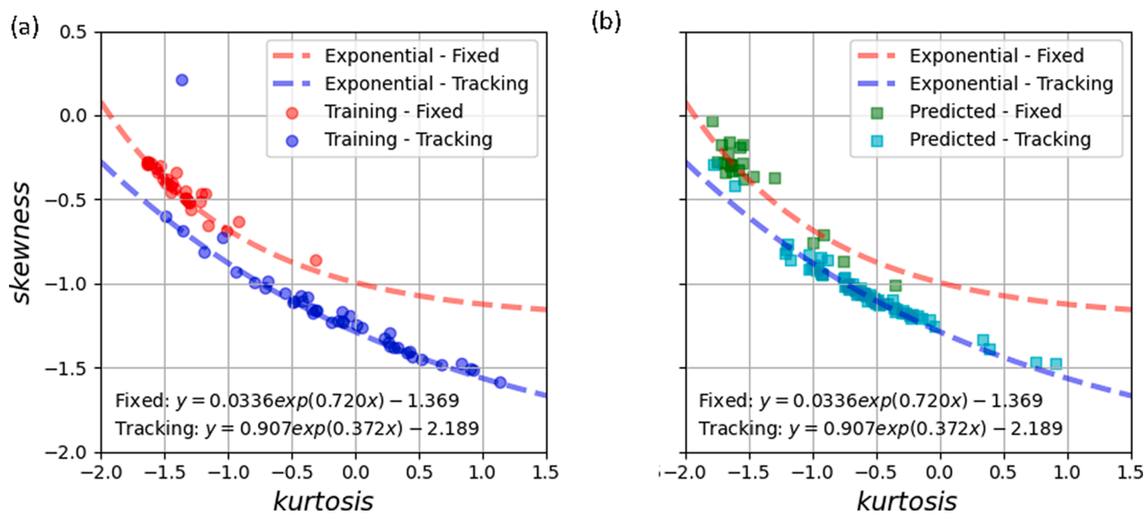

Fig. 6. Plotting of *kurtosis* vs *skewness* extracted from P90 AVG-TDPs of each PV system: (a) training and (b) prediction, with the extracted exponential lines for Fixed and Tracking systems from training.

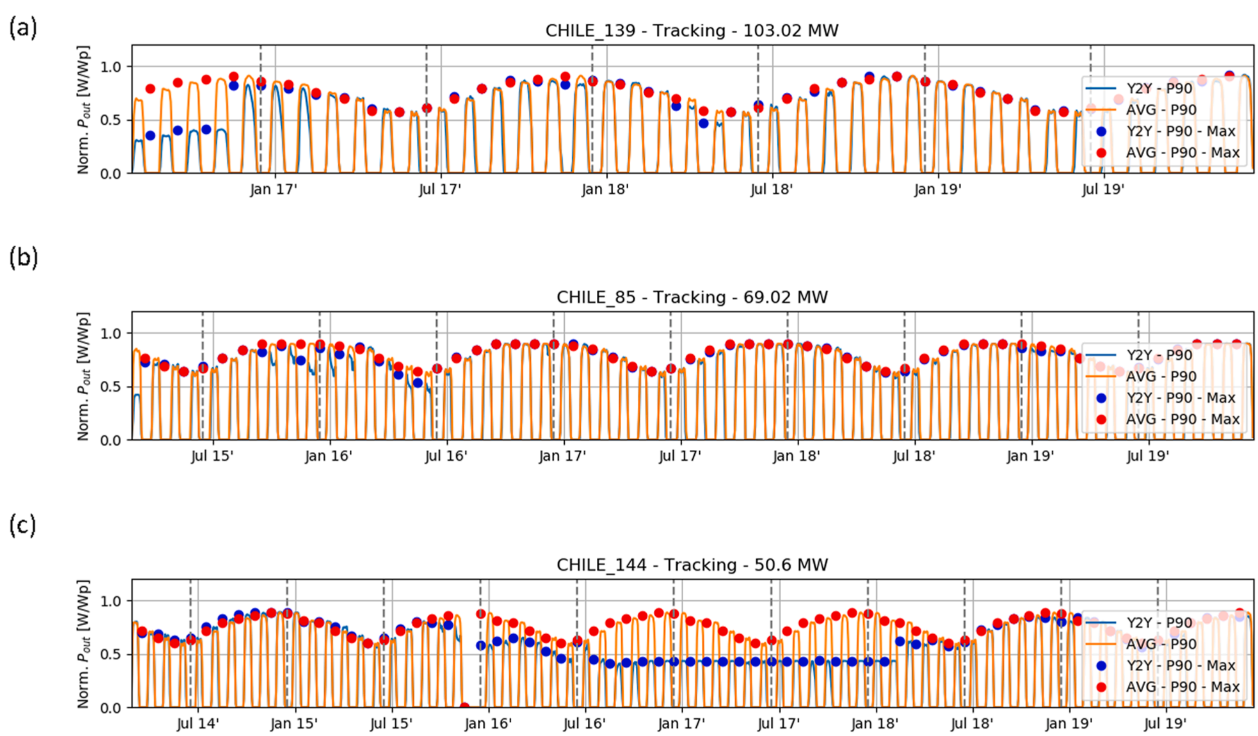

Fig. 7. Comparison of P90 AVG-TDPs and P90 Y2Y-TDPs on PV systems. (a) CHILE_139: identification of initial operational phases. (b) CHILE_85: curtailment during the years 2015 and 2016. (c) CHILE_144: failure in 2015, followed by large performance losses during the years 2016 and 2017.

2019. This identification of mounting configuration is also used to extract more statistics in the current PV performance assessment.

4.5. Year-to-Year TDP of PV systems' output power

The power output of PV systems is directly related to the solar irradiance reaching their surface. In optimal conditions, the power output can be mostly related to irradiance data measured by a pyranometer installed on-site, and in less manner thermal, spectral and incident angle factors. However, the long-term operation of PV systems largely depends on temporal events and performance losses caused by weather phenomena, component failures or poor maintenance. As mentioned above, using a percentile 90th on TDPs can help to neglect underperformance periods for the evaluation of the PV performance without external factors. One of the temporal events for large-scale PV systems can be defined as the "initial operational phase", which indicates a gradual increase of power output to nominal during the first months after the grid connection, and it is observed as common practice for the integration of very large PV systems (Jäger-Waldau, 2019). In practice, an example of this is evidenced in CHILE_139 (see Fig. 7.a), which entered in operation in different phases (Informe de Auditoría DO PES Quilapilún, 2020).

Another temporal event is the "curtailment" of power injection due to limitations applied by the grid operator. The performance of Chile_85 was affected by this issue, as observed in Fig. 7.b. The daily profile under curtailment agrees with the one presented in (Zurita et al., 2018) and coincides with the periods reported in (PV Tech.org, 2016).

The comparison of P90 Y2Y-TDP and P90 AVG-TDP can visually reflects "large performance losses" due to conversion unit failures. A clear example of this factor is observed in the power production of Chile_144 (Fig. 7.c), which had to be reconstructed due to severe damage after

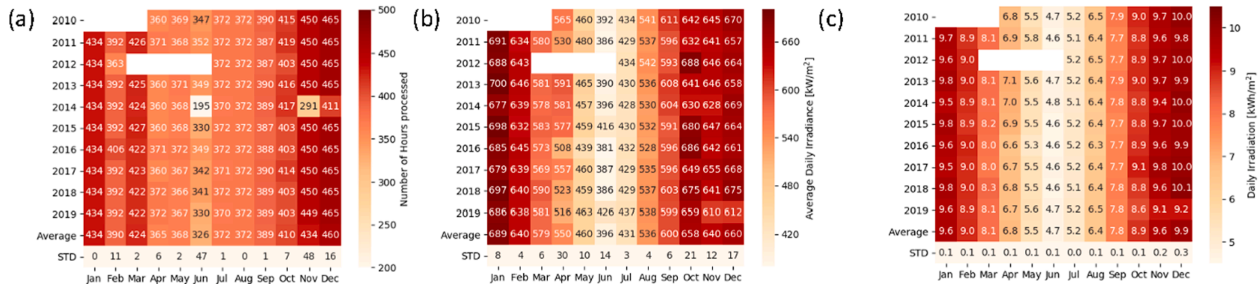

Fig. 8. Results based on P90 Y2Y-TDP calculations for *GHI* in the weather station IDEO. (a) Number of hours processed, (b) Average daily irradiance in W/m^2, and (c) Daily global horizontal irradiation in kWh/m^2.

alluvium, keeping production at less than half for around 18 months.

Other issues such as "inverter clipping", "missing data", and "outliers" could also be visually recognised from the TDPs. The TDPs of each PV system are given in *Supplementary Materials*.

4.6. Sensitivity analysis of Y2Y-TDPs

To evaluate the long-term variability of the TDP approach (i.e., Y2Y-TDPs), solar irradiance measurements can be used due to their representativeness of a PV system in optimal conditions (e.g., a quasi-linear relationship between irradiance and PV power).

Fig. 8.a illustrates the number of hours used to process the TDP per month in the weather station IDEO. During summertime (from December to February in the southern hemisphere), the useful number of hours processed can get up to 465 h, while in wintertime, it gets close to 326 h. When data issues occur, partial or full data loss is directly reflected in the visualization (see the month of June and November 2014 in Fig. 8.a).

The daily average irradiance ranges from 381 W/m^2 to 700 W/m^2 (see Fig. 8.b). In this case, the partial data loss is not reflected in the values. The annual variability, or standard deviation (STD), goes from 3 W/m^2 to 30 W/m^2, confirming a low variability of the TDP approach for long-term solar irradiance analysis.

Finally, the P90 Y2Y-TDP of the daily irradiation (the sum of the typical daily profiles) is presented in Fig. 8.c. Here the variability ranges from 0 to 0.3 kWh/m^2 absolutely, and 1.5% to 3.0% relatively, which confirms that the TDP approach has a very low annual solar variability and low sensitivity to anomalies.

4.7. Key performance indicators based on Typical Daily Profiles

The main PV performance indicators are defined in IEC 61724-1 (International Electrotechnical Comission). However, since the parameters at STC conditions are unknown in our case study, the indicators would be calculated considering the net power (P_{net}) instead of the rated STC power.

Thus, the essential performance indicators utilised in this work are: the reference yield (Y_r), the net injected energy yield (Y_{net}), the net Unit Capacity Factor (UCF_{net}) and the net Performance Ratio (PR_{net}). As shown in Equations (3)–(5): the Y_r is defined as the cumulative incident irradiance (G) in a certain period (t) divided by 1000 W/m^2 (G_0); the Y_{net} is the energy injected to the grid (E_{net}) in a certain period divided byP_{net}; the PR_{net} as the ratio of Y_{net} and Y_r; finally, the UCF_{net} characterises the availability of the annually produced energy (Ascencio-Vásquez et al., 2019) and is calculated by dividing annual Y_{net} by 8760 h (see Eq. (6)).

$$Y_r = \frac{\int_{t_1}^{t_2} G(t)}{G_0} \quad (1)$$

$$Y_{net} = \frac{E_{net}}{P_{net}} \quad (2)$$

$$PR_{net} = \frac{Y_{net}}{Y_r} \quad (3)$$

$$UCF_{net} = \frac{Y_{net}}{8760\mathrm{h}} \quad (4)$$

To obtain the Y_r of each PV plant, the P90 AVG-TDP was used to identify the type of mounting structure (Section 4.4), and then the incident irradiance (G) for fixed and tracking mounting conditions were modelled (refer to Section 3.3.2). To obtain the Y_{net}, the E_{net} was calculated by the power production time-series and theP_{net} extracted from (Comision Nacional de Energia (CNE) Chile, 2020b). To reduce uncertainties in the available data, a filter stage neglects data with *GHI* below 500 W/m^2, and PR_{net} below 0.5 and above 1.2.

5. Results

In this section, the TDP approach for PV performance assessment is applied to the 2.6GW large-scale PV systems in Chile. Firstly, the modelling and validation of the solar irradiance for fixed and tracking PV systems are presented, followed by the validation of the PV performance assessment using high accuracy data retrieved from neighbouring PV systems and weather stations. Finally, the whole portfolio is evaluated at the country level.

5.1. Modelling and validation of the solar irradiance.

5.1.1. Modelling for fixed and tracking PV systems

From *GHI*, Diffuse Horizontal Irradiance (*DHI*) and Direct Normal Irradiance (*DNI*) are estimated using the Erbs decomposition model (Erbs et al., 1982), while the Hay-Davies transposition model (Hay and Davies, 1980) is utilised to calculate the irradiance on tilted or tracked plane of array surfaces.

For Fixed PV systems, the incident irradiance is mentioned as Global Plane-of-Array Irradiance (G_{PoA}) and the tilt angle estimated as a function of the Latitude (Jacobson and Jadhav, 2018).

For Tracking PV systems, the incident irradiance is referred to as Global Tracking Irradiance (G_{Track}) and the daily tracking goes from East to West with a flat position at solar noon. Additionally, ground coverage ratio (*GCR*) of 0.33, backtracking and maximal angle tracking of 90° are considered. The sun tracking algorithm is available in (Lorenzo et al., 2011; Stein et al., 2016).

5.1.2. Validation of modelled tracking irradiance data

The validation of the *GHI* extracted from ERA5 and the modelled G_{Track} (ERA5 + PVLib) can be performed thanks to the available irradiance measurements at the eleven weather stations (refer to Section 3.3.2). Uncertainties at three modelling steps are evaluated: uncertainty in the modelled *GHI* data; uncertainty due to the decomposition and transposition model; and total modelling uncertainty between measured and modelled G_{Track}. The evaluation includes Cumulative Distribution functions (CDFs) and three statistical indicators: Coefficient of determination (R^2), root-

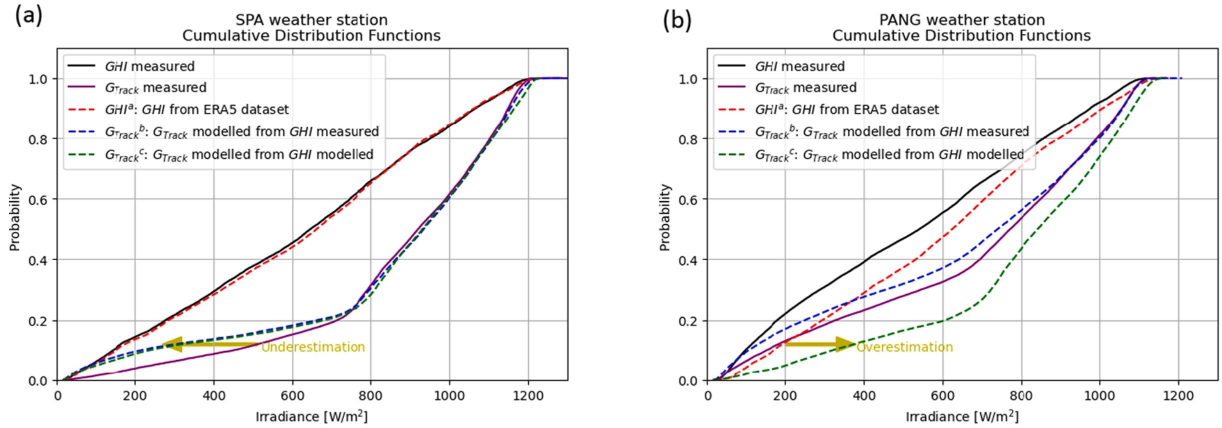

Fig. 9. (a) CDF plots for the weather station SPA. (b) CDF plots for the weather station PANG.

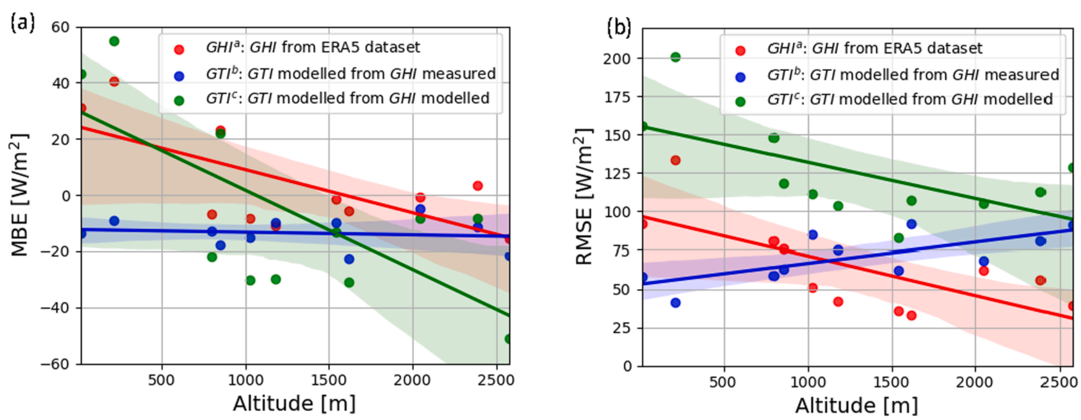

Fig. 10. (a) MBE and its trend versus altitude. (b) RMSE and its trend versus altitude.

mean-square-error (RMSE) and the mean-bias-error (MBE). As follows, only the best (SPA station) and worst (PANG station) matching cases are discussed. The statistical indicators for the other nine stations are given in Appendix C.

The CDF plot helps to identify the modelling accuracy at different irradiance levels. At the SPA station (Fig. 9.a), excellent agreement is observed at all levels of *GHI*, ensuring that data from ERA5 can be reliably used at the location. Also, the modelling of G_{Track} from measured

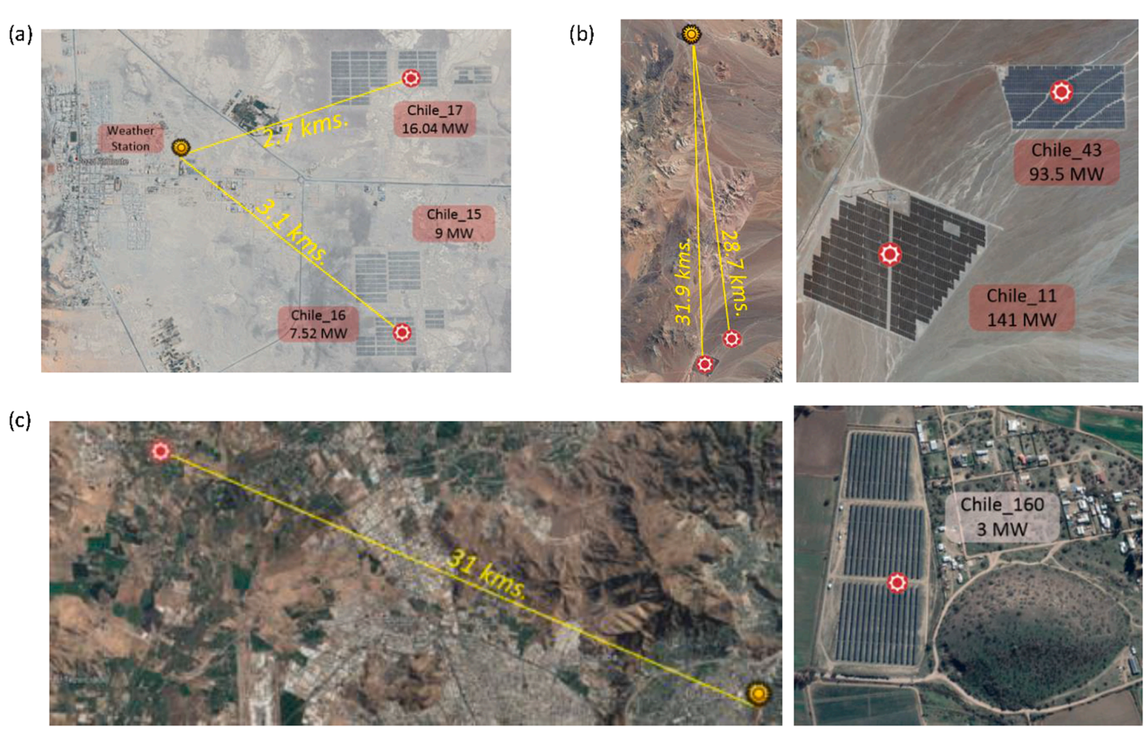

Fig. 11. Neighbouring PV systems and weather stations. (a) Weather station PALM and PV systems CHILE_16 and CHILE_17. (b) Weather station IDEO and PV systems CHILE_11 and CHILE_43. (c) Weather station CCA and the PV system CHILE_160 (Source: Google Earth Pro).

Table 3
Net Performance Ratio of four PV systems under different approaches.

Weather Station	PV system	Net Power [MW]	PR_{net}[%] using measured Irradiance		PR_{net}[%] using modelled Irradiance	
			Common Practice	P90 AVG-TDP	Common Practice	P90 AVG-TDP
IDEO	CHILE_11	141.00	80.11	80.45	78.10	79.33
	CHILE_43	93.50	76.38	77.62	74.56	76.65
PALM	CHILE_16	7.52	84.00	83.99	83.33	82.49
	CHILE_17	16.04	86.68	84.13	84.23	82.65
CCA	CHILE_160	3.00	83.74	85.79	79.13	82.71

Table 4
Summary of temporal events through long-term P90 TDPs in Chilean large-scale PV systems.

Events	Number of systems	Percentage
Initial progressive rated capacity	>15	>8.9%
Curtailment	>12	>7.1%
Large performance losses	>29	>17.3%
Inverter Clipping	>93	>55.4%
Missing data	42	25.0%
No useful data	8	4.8%

GHI agrees with the measured G_{Track}. The global uncertainty of modelled G_{Track} using *GHI* from ERA5 shows good agreement above 700 W/m^2. The underestimations below 700 W/m^2 can be attributed to the decomposition model. At the PANG station (Fig. 9.b), large deviations are already observed in the *GHI* extracted from ERA5. Also, deviations due to decomposition and transposition models are reflected in the CDFs of modelled G_{Track} from measured *GHI* and measured G_{Track}. Both uncertainties combined are the reason for a considerable deviation between the modelled and measured G_{Track}.

The statistical indicators RMSE and MBE help to identify and quantify deviations and under-or over-estimations. By correlating the indicators with the altitude of each weather station, it is possible to observe larger deviations and overestimations at low altitudes (e.g., below 1000 m) and underestimations at high altitudes (e.g., above 1000 m). This issue can be seen in Fig. 10.a and 10.b, and it could be related to the reported cloud modelling deviations (Jiang et al., 2020). Also, the figures help to identify underestimations due to the chosen decomposition and transposition models, where larger deviations for locations occur at high altitudes.

The results presented in this section and in Appendix C give a comprehensive validation of the irradiance modelling carried out. In specific, the G_{Track} modelled using *GHI* from ERA5 shows small deviations (±30 W/m^2) at the altitudes from 500 m to 2000 m, where most of the PV systems are installed. This aspect helps to justify the use of the modelled tracking irradiance data in the PV performance assessment, which is presented and discussed later.

5.2. KPIs on neighbouring PV systems and weather stations

The clusters among the PV systems and weather stations are used to validate the TDP approach using high-quality irradiance sensors. In this regard, three cases have been identified: (1) PV systems CHILE_16 (Tracking, 7.52 MW) and CHILE_17 (Tracking, 16.04 MW) located at around 3 km of the weather station PALM (Fig. 11.a); (2) PV systems CHILE_11 (Tracking, 141 MW) and CHILE_43 (Tracking, 93.5 MW) located at around 30 km of the weather station IDEO (Fig. 11.b); (3) CHILE_160 has 3 MW rated power, and it is installed 31 km away of CCA weather station (Fig. 11.c).

The performance indicators are presented in Table 3. Deviations in PR_{net} are mainly due to differences in the irradiance data used as input. In CHILE_11, the deviations are mainly due to different stages of rated power during the early months of operation.

5.3. Analysis of PV systems in Chile using the TDP approach

5.3.1. Observation of temporal events

The P90 AVG-TDP, first, was used to identify the type of mounting structure for all PV plants. Then, the incident irradiance for fixed and tracked mounting was modelled to obtain the reference yield for each PV system. Then, the P90 Y2Y-TDP was used to simplify the raw data of PV energy production and exclude temporal events – such as failures, missing data, curtailment, and poor O&M activities, among others – which can increase uncertainty in the PV performance assessment. Finally, the TDP approach is used to calculate three performance indicators: the net injected energy yield (Y_{net}), the annual Unit Capacity Factor (UCF_{net}) and the net Performance Ratio (PR_{net}).

The key performance indicators of each PV system, as well as the P90AVG-TDP and P90 Y2Y-TDP, are given in *Supplementary Materials*. Visual observation of the long-term time-series of power production generated using the TDP approach, five temporal events are detected and manually classified (see Table 4). The largest PV systems (above 20 MW installed capacity) show a progressive increase of rated power during the first years of operation (at least 15) and curtailment (at least 12). Long periods with remarkable underperformances (e.g., inverter failures, tracking failures, string disconnections, etc.) were identified in at least 29 PV systems. Operation under inverter clipping is observed in at least 93 PV systems. Gaps in the operational data (e.g., communication issues or total production shutdown) were detected in 45 PV systems. Finally, 8 out of 168 PV systems do not have useful data to run the PV performance assessment.

5.3.2. Calculation of operational key performance indicators

Fig. 12.a shows the quantity of PV systems for Fixed and Tracking structures at different levels of net power. The largest PV system in Chile reaches 200 MW net power. Eight PV systems are larger than 100 MW, 18 PV systems between 25 and 100 MW, while 141 PV systems report a net power below 25 MW.

The UCF_{net} is presented in Fig. 12.b, where considering PV systems older than one year of operation, it is possible to see three systems with UCF_{net} higher than 0.35 for solar tracking systems. The abundant solar resource in the central and northern regions allows UCF_{net} larger than 0.20 – reaching a total of 89 PV plants.

In terms of energy yield (kWh/kW$_p$), Fig. 12.c shows that the average of fixed systems in Chile is even double than the one in some European countries. For tracking systems, the annual yield is considerably higher than similar systems installed in Spain. A remarkable number of PV systems (28) present a yield higher than 2500 kWh/kW$_p$, proving an excellent opportunity for PV deployment.

Fig. 12.d correlates the energy yield and net performance rate for both fixed and tracking systems with at least one year of operation. By increasing the annual energy yield, the performance ratio also increases, getting even above 85%. Finally, in Fig. 12.e, the geographical distribution of the net performance ratio is illustrated, but no clear pattern regarding regions is recognised.

6. Discussion

The diverse geography of the country (different climate zones) proofs that Chile can be an attractive natural laboratory for PV technologies,

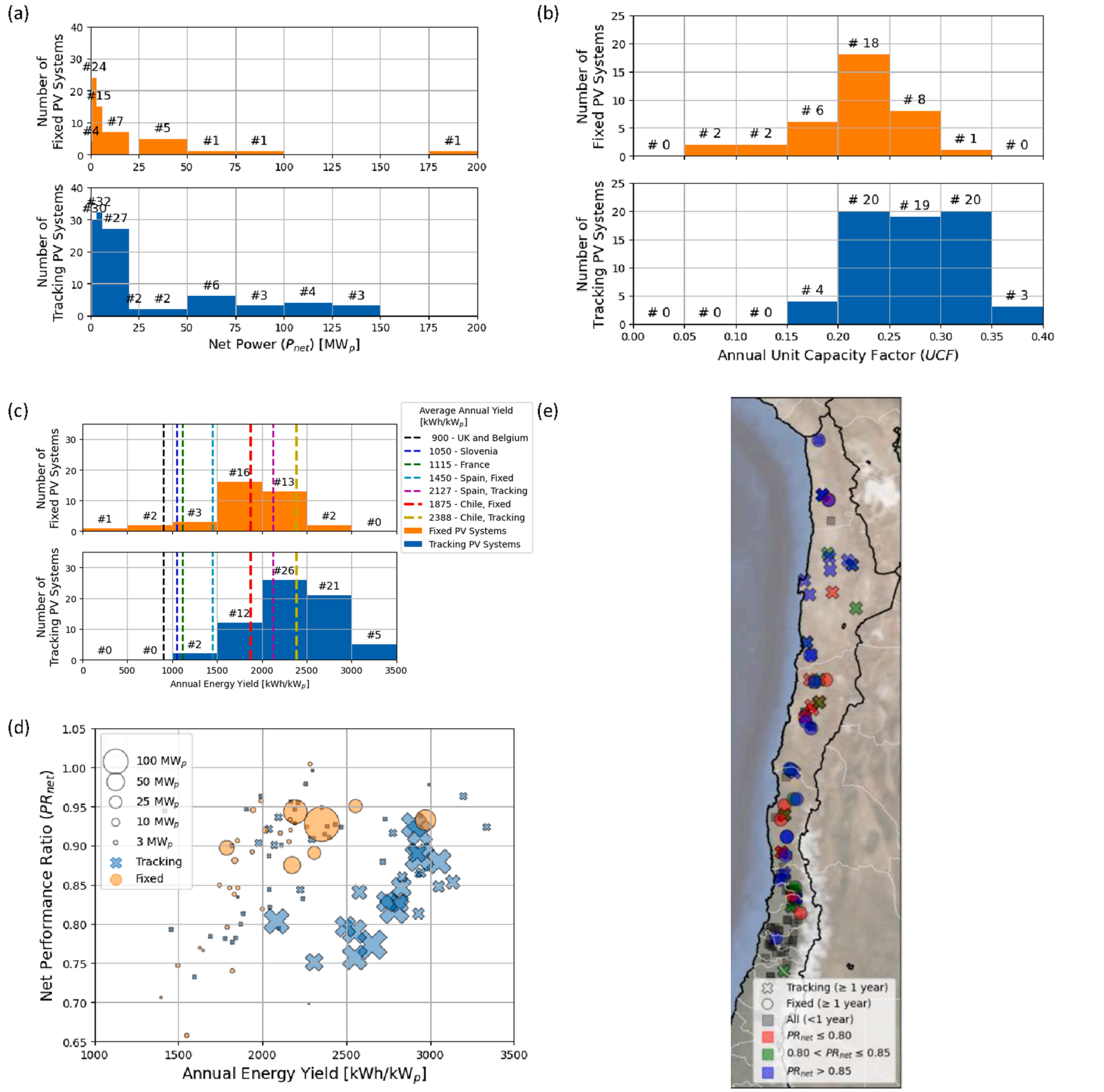

Fig. 12. (a) Number of projects and installed PV capacity. (b) Annual Unit Capacity Factor of PV systems under at least one year of operation. (c) Annual energy yield of PV systems under at least one year of operation. (d) Correlation of annual energy yield and net performance serious, indicating the mounting configuration and size of PV systems. (e) Geographical distribution of the net performance ratio for systems under at least one year of operation.

and preliminary research already shows promising results (ATAMOS-TEC, 2020). The Atacama Desert has the highest solar irradiation in the World, the Central area presents high irradiation in a temperate climate, and in the Southern regions, the similarity of annual irradiation with European countries are observed.

The TDP approach was applied to a fleet of 168 PV systems operating in Chile and validated on five PV systems with neighbouring weather stations. Even though the TDP can help to identify the most-like mounting condition, essential details such as the exact tilt and azimuth angle in fixed structures, and specific characteristics of rotation axis for tracking systems, cannot be extracted. The TDP approach allows evaluation of PV performance for larger fleets, as it was used here at the country level processing data at the grid injection point, combined with modelled weather data based on climate reanalysis datasets.

The TDP approach also shows the potential to be applied to both fixed and tracking PV systems. The simplified model helps to reduce the calculation uncertainties due to singular performance losses such as O&M activities, inverter failures, missing data, among others. The periodical analysis of the PV energy production provided by the "Energía Abierta" tool can give interesting insights into the status of PV systems in the country and provide new information to reduce the risk of future investments. This new methodology could also be useful to identify orientation mounting for all kinds of PV systems, from ground installation to Building Integrated Photovoltaic (BIPV) systems. Having longer time series in the future, the performance loss and degradation rate of PV systems could complement the current PV performance assessment and help to optimise the material selections at specific climate zones.

An aspect to consider in future works is the impact of temperature on the time series generated with the TDP. While extracting the P90 TDP for power and irradiance will result in a very realistic clear-sky day profile, the P90 TDP for temperature could present the worst and even an unrealistic scenario, which could overestimate the thermal losses. The same aspect should be carefully considered when analysing PV systems operating in locations with a high presence of soiling and snow.

The TDP approach is recommended for short (a year or less) and long time series (several years). The main outcome at analysing short time-series could be focused on the performance losses during clear sky days and rated values. On the other hand, for long-term time series, system interruptions, degradation, curtailment, among others, could be the focus of more in-depth analysis, like the one presented in this article.

7. Conclusions

In this study, a new approach called Typical Daily Profiles (TDP) has been developed due to the necessity of new methods for PV performance assessments on large PV fleets or at the country level. To extract most KPIs for PV systems, current methods require accurate operational data and historical events and technical interventions. However, they are usually not publicly available. Thus, the challenge to analyse the performance of an extensive portfolio of large-scale PV systems with minimal information has been addressed. To achieve the extraction of performance indicators, the use of the novel TDP methodology was presented. The performance assessment of 168 PV systems operating in Chile using the TPD approach is reported.

The TDP approach provides a tool to identify the mounting condition of a PV system based on statistical indicators (kurtosis and skewness). Two exponential equations can help to differentiate and label fixed and tracking mounted PV systems. The results have shown a dominance of tracking systems in Chile (around 65% of 168 PV systems). This tendency is justified by the large energy yield (average of 2388 kWh/kW_p) and unit capacity factor (up to 38% on an annual basis).

Also, the TDP approach is used to evaluate the operation of PV systems by providing clear visualizations for the identification of specific events such as curtailment (7.1% of PV systems evaluated), large performance losses (17.3%), inverter clipping (55.4%) and missing data (25.0%). The final calculations show net performance ratio values over 75% under optimal conditions and up to 100% for tracking systems with oversizing at DC side (noted by the inverter clipping in summer). In the future, periodical performance assessment using TDP can help to provide information about the current PV systems and reduce the risk of further investments.

Finally, the geography of Chile offers high solar irradiation in most of the regions, notably the highest in the World in the Atacama Desert. The installation of tracking structures can increase the energy yield and unit capacity factor considerably. Chile has a great solar potential to accelerate the electrical transition from conventional to renewable sources, where the PV industry is expected to have a crucial role in the energy matrix.

Declaration of Competing Interest

The authors declare that they have no known competing financial interests or personal relationships that could have appeared to influence the work reported in this paper.

Acknowledgements

The authors would like to thank the organisations ECMWF, MINENERGIA, CNE for given free access to operational datasets.

This project has received funding from the European Union's H2020 programme SOLAR-TRAIN under grant agreement No 721452, research programme P2-0197 funded by Slovenia Research Agency, and the Vice-Rectorate of Research of the University of Jaén for the "Acción 4" scholarship: "Ayudas predoctorales para la Formación de Personal Investigador".

Author contributions

J.A-V. worked on the conceptualisation, data processing, visualizations, simulations, analyses and writing the manuscript. J.C.O-A worked on the presentation of the published work, specifically writing the initial draft as well as commenting and reviewing pre-or post-publication stages. K.B. and M.T. help in conceptualisation, discussed the results and reviewed the manuscript. E.M-C supported the preparation of the published work, specifically with a critical review of the final draft. All the authors discussed the results and contributed, read and commented the manuscript.

Appendix A. Irradiance range per region

Table A1.

Table A1
Average annual irradiation, minimum and maximum for plotting, name and code per region.

Name ISO 3166-2:CL	Number ISO 3166-2:CL	Code ISO 3166-2:CL	Average per Region [kWh/m^2]	Minimum for plotting [kWh/m^2]	Maximum for plotting [kWh/m^2]
Antofagasta	II	CL-AN	2612.55	3000.00	2576.50
Atacama	III	CL-AT	2540.46	2576.50	2535.99
Tarapacá	I	CL-TA	2531.52	2535.99	2494.44
Arica y Parinacota	XV	CL-AP	2457.35	2494.44	2387.26
Coquimbo	IV	CL-CO	2317.17	2387.26	2242.55
Valparaíso	V	CL-VS	2167.93	2242.55	2157.97
Metropolitana	XIII	CL-RM	2148.01	2157.97	2098.17
O'Higgins	VI	CL-LI	2048.33	2098.17	2026.54
Maule	VII	CL-ML	2004.76	2026.54	1936.24
Biobío, Ñuble	VIII, XVI	CL-BB, -NB	1867.73	1936.24	1772.45
La Araucanía	IX	CL-AR	1677.17	1772.45	1589.94
Los Ríos	XIV	CL-LR	1502.72	1589.94	1442.50
Los Lagos	X	CL-LL	1382.27	1442.50	1291.53
Aysén	XI	CL-AI	1200.79	1291.53	1116.34
Magallanes	XII	CL-MA	1031.88	1116.34	900.00

Appendix B. Performance indicators of large-scale PV Systems in Chile

Short_Name	Lat.	Lon.	MC	Pnet	UCFn	Yfn	PRn	Short_Name	Lat.	Lon.	MC	Pnet	UCFn	Yfn
CHILE_1	−24.0	−68.6	T	21.8	0.3345	2931	0.813	**CHILE_44**	−32.9	−70.7	T	2.7	0.1347	1173
CHILE_2	−33.9	−71.6	F	3.0	0.1792			**CHILE_45**	−32.7	−70.6	T	3.0	0.2076	1732
CHILE_3	−22.4	−68.9	F	9.0				**CHILE_46**	−36.4	−72.4	T	1.5	0.2624	2298
CHILE_4	−22.8	−69.5	T	99.1	0.3483	3051	0.879	**CHILE_47**	−36.4	−72.4	T	1.5	0.2507	2182
CHILE_5	−23.5	−69.4	T	138.2	0.3031	2653	0.773	**CHILE_48**	−31.8	−71.0	F	3.0	0.1144	1002
CHILE_6	−20.5	−69.5	F	26.7	0.0564	418	0.868	**CHILE_49**	−34.1	−70.8	F			
CHILE_7	−20.5	−69.5	F	26.7	0.2636	2309	0.891	**CHILE_50**	−26.4	−70.1	T	36.0	0.2943	2576
CHILE_8	−20.4	−69.5	F	3.0	0.1769	1548	0.657	**CHILE_51**	−34.8	−71.0	T	3.0	0.1929	1690
CHILE_9	−27.6	−70.3	F	3.0	0.2464	2056	0.905	**CHILE_52**	−31.7	−71.1	F	2.9	0.2215	1940
CHILE_10	−27.1	−70.2	T	101.0	0.2912	2548	0.757	**CHILE_53**	−33.6	−70.9	F	2.8		
CHILE_11	−27.0	−69.9	T	141.0	0.3181	2738	0.819	**CHILE_54**	−25.5	−70.2	T	104.0	0.3355	2936
CHILE_12	−22.2	−69.6	T	68.0	0.3228	2828	0.847	**CHILE_55**	−35.2	−71.1	T	1.3	0.2116	1853
CHILE_13	−22.3	−69.5	T	138.0	0.3353	2937	0.885	**CHILE_56**	−34.5	−71.5	T	2.9	0.1295	1132
CHILE_14	−23.1	−70.4	T	6.2	0.3103	2718	0.879	**CHILE_57**	−32.8	−70.9	T	3.0	0.1402	1227
CHILE_15	−20.3	−69.8	T	9.0	0.3651	3198	0.963	**CHILE_58**	−31.7	−71.2	T	3.0	0.2101	1839
CHILE_16	−20.3	−69.8	T	7.5	0.3344	2930	0.863	**CHILE_59**	−26.4	−70.0	F	28.1	0.2917	2409
CHILE_17	−20.3	−69.8	T	16.0	0.3362	2945	0.865	**CHILE_60**	−34.3	−71.4	T	3.0	0.233	2040
CHILE_18	−22.4	−68.9	T	9.0	0.2327	2036	0.921	**CHILE_61**	−32.5	−71.3	F	34.6	0.2041	1787
CHILE_19	−23.5	−70.4	F	0.6	0.2598	1647	0.698	**CHILE_62**	−34.3	−71.0	T	7.5	0.0882	773
CHILE_20	−22.4	−68.9	T	9.0	0.3809	3334	0.924	**CHILE_63**	−32.9	−71.2	F	3.0	0.2274	1991
CHILE_21	−29.4	−71.0	T	2.0	0.2255	1965	0.939	**CHILE_64**	−36.3	−71.9	T	3.0	0.2579	2258
CHILE_22	−30.2	−71.1	F	1.3	0.1857	1624	0.769	**CHILE_65**	−30.8	−71.1	T	3.0	0.3359	2942
CHILE_23	−18.4	−69.9	F	2.0	0.023	201	0.916	**CHILE_66**	−33.7	−71.0	T	7.3	0.1253	1097
CHILE_24	−18.4	−69.9	F	2.0	0.2587	2266	0.924	**CHILE_67**	−29.1	−70.9	T	100.0	0.3314	2898
CHILE_25	−22.6	−68.7	T	32.1	0.3579	3135	0.853	**CHILE_68**	−34.8	−71.1	T	2.9	0.2504	2187
CHILE_26	−22.6	−68.7	T	22.5	0.3483	3051	0.848	**CHILE_69**	−26.3	−69.7	F	3.0	0.0824	548
CHILE_27	−26.3	−69.6	F	3.0	0.2079	1598	0.740	**CHILE_70**	−33.6	−71.2	T	3.0	0.2725	2385
CHILE_28	−29.1	−70.9	F	3.0	0.2283	1994	0.819	**CHILE_71**	−36.0	−71.7	F	3.0	0.2405	2106
CHILE_29	−32.9	−70.7	T	3.0	0.282	2467	0.924	**CHILE_72**	−32.4	−71.0	T	3.0	0.2239	1960
CHILE_30	−32.4	−70.9	F	3.0	0.1992	1700	0.849	**CHILE_73**	−34.2	−71.4	F	6.9	0.0272	236
CHILE_31	−33.1	−70.8	F	3.0	0.0817	686	0.695	**CHILE_74**	−34.0	−71.4	T	8.8	0.2365	2070
CHILE_32	−30.6	−71.2	F	6.0	0.2095	1834	0.881	**CHILE_75**	−29.1	−70.9	F	196.0	0.2687	2352
CHILE_33	−30.6	−71.3	T	3.0	0.2396	2097	0.794	**CHILE_76**	−34.1	−71.4	T	3.0	0.2412	2112
CHILE_34	−27.5	−70.4	T	9.0	0.3171	2778	0.916	**CHILE_77**	−32.7	−70.7	T	9.0	0.1332	1166
CHILE_35	−32.3	−71.3	T	3.0	0.0883	773	0.767	**CHILE_78**	−33.8	−70.7	F	1.5	0.074	648
CHILE_36	−31.7	−71.2	T	3.0	0.1663	1431	0.793	**CHILE_79**	−34.0	−71.3	F	8.9	0.1713	1456
CHILE_37	−31.7	−71.2	F	3.0	0.1642	72	1.016	**CHILE_80**	−32.7	−70.7	F	2.5	0.206	1804
CHILE_38	−32.5	−71.1	F	3.0	0.2092	1832	0.838	**CHILE_81**	−27.7	−70.2	F	0.4	0.0494	311
CHILE_39	−27.8	−70.1	T	9.0	0.2483	2173	0.916	**CHILE_82**	−21.1	−69.5	T	98.0	0.1574	1364
CHILE_40	−32.9	−70.6	T	3.0	0.2179	1907	0.940	**CHILE_83**	−31.6	−71.1	F	3.0	0.1154	1011
CHILE_41	−31.7	−71.1	T	3.0	0.1165	1021	0.923	**CHILE_84**	−32.5	−71.3	F	3.0	0.046	402
CHILE_42	−27.5	−70.4	F	0.4	0.1253	1097	0.648	**CHILE_85**	−26.3	−70.2	T	69.0	0.2849	2493
CHILE_43	−27.0	−69.9	T	93.5	0.291	2546	0.790	**CHILE_86**	−34.9	−71.0	T	1.3	0.0844	739

PRn	Short_Name	Lat.	Lon.	MC	Pnet	UCFn	Yfn	PRn	Short_Name	Lat.	Lon.	MC	Pnet	UCFn	Yfn	PRn
0.868	**CHILE_87**	−34.5	−71.1	T	8.4	0.0859	587	0.811	**CHILE_130**	−32.8	−70.8	F	6.0	0.2304	2018	0.920
0.900	**CHILE_88**	−34.0	−71.7	T	9.0	0.1559	1326	0.901	**CHILE_131**	−32.8	−70.9	T	3.0	0.1479	1295	0.930
0.996	**CHILE_89**	−30.5	−71.1	T	2.9	0.2078	1821	0.777	**CHILE_132**	−35.0	−71.7	T	3.0	0.2526	2211	0.955
0.928	**CHILE_90**	−34.3	−71.5	T	9.0	0.2393	2012	0.936	**CHILE_133**	−34.2	−71.8	F	2.8			
0.827	**CHILE_91**	−34.8	−71.8	F	4.8	0.222	1944	0.946	**CHILE_134**	−33.3	−71.4	T	3.0	0.2328	1965	0.887
	CHILE_92	−34.6	−71.4	T	6.9	0.162	1378	0.968	**CHILE_135**	−33.7	−70.6	T	2.7	0.1557	1321	0.895
0.840	**CHILE_93**	−32.4	−71.2	F	3.0	0.0329	208	0.872	**CHILE_136**	−34.6	−71.1	T	9.0	0.0087	61	
0.784	**CHILE_94**	−33.9	−71.6	F	3.0	0.1709	1496	0.747	**CHILE_137**	−34.5	−71.5	T	2.9	0.1319	1152	0.879
0.892	**CHILE_95**	−33.0	−70.7	T	3.0	0.2738	2397	0.911	**CHILE_138**	−34.3	−71.6	T	3.0	0.2153	1853	0.813
	CHILE_96	−29.2	−70.7	T	1.5	0.342	2991	0.978	**CHILE_139**	−33.1	−70.7	T	103.0	0.2379	2082	0.803
0.916	**CHILE_97**	−30.5	−71.1	T	3.0	0.2559	2240	0.832	**CHILE_140**	−33.9	−71.4	T	3.0	0.0733	642	0.775
0.834	**CHILE_98**	−25.1	−70.3	T	55.0	0.3216	2813	0.826	**CHILE_141**	−34.8	−71.8	T	2.9	0.0831	728	0.810
0.877	**CHILE_99**	−25.1	−70.3	T	16.5	0.3235	2829	0.860	**CHILE_142**	−32.8	−71.0	T	3.0	0.2136	1806	0.800
0.949	**CHILE_100**	−36.5	−72.0	T	3.0	0.1251	1095	0.977	**CHILE_143**	−34.6	−71.2	T	7.0	0.147	1287	0.939
0.782	**CHILE_101**	−36.5	−72.1	T	3.0	0.1141	999	0.972	**CHILE_144**	−27.3	−70.1	T	50.6	0.2636	2307	0.751
0.950	**CHILE_102**	−30.7	−71.2	F	2.9	0.2044	1790	0.796	**CHILE_145**	−33.0	−70.7	T	3.0	0.2706	2369	0.915
0.844	**CHILE_103**	−36.8	−72.2	T	3.0	0.2273	1904	0.963	**CHILE_146**	−34.3	−70.8	F	2.7	0.0211	185	0.529
0.897	**CHILE_104**	−35.4	−71.6	T	3.0	0.0987	865	0.829	**CHILE_147**	−33.9	−71.4	F	3.0	0.2113	1850	0.906
0.889	**CHILE_105**	−33.8	−71.3	T	3.0	0.1619	1379	0.944	**CHILE_148**	−33.7	−71.0	T	3.0	0.0576	463	0.781
0.957	**CHILE_106**	−33.3	−70.9	F	3.0	0.103	892	0.850	**CHILE_149**	−30.6	−71.4	T	2.7	0.1697	1480	0.946
0.979	**CHILE_107**	−34.0	−71.3	F	2.9	0.0954	835	0.842	**CHILE_150**	−32.3	−71.1	T	3.0	0.2778	2432	0.927
0.938	**CHILE_108**	−33.0	−70.8	F	1.1	0.1595	1392	0.706	**CHILE_151**	−32.4	−71.0	T	3.0	0.203	1625	0.781
0.823	**CHILE_109**	−36.0	−71.8	T	3.0	0.2476	2168	0.956	**CHILE_152**	−33.1	−70.9	F	90.8	0.2508	2194	0.943
0.926	**CHILE_110**	−34.1	−70.8	F	8.0	0.1317	1064	0.915	**CHILE_153**	−30.0	−70.7	F	3.0	0.2472	2164	0.933
0.947	**CHILE_111**	−27.9	−70.2	F	46.0	0.2485	2173	0.875	**CHILE_154**	−35.5	−71.6	F	9.0	0.1008	883	0.919
0.809	**CHILE_112**	−35.3	−71.6	T	3.0	0.2093	1732	0.961	**CHILE_155**	−30.6	−71.3	T	3.0	0.3117	2729	0.934
0.924	**CHILE_113**	−33.9	−71.6	T	2.7	0.0609	534	0.897	**CHILE_156**	−33.1	−70.8	T	3.0	0.1821	1595	0.732
0.916	**CHILE_114**	−34.0	−70.6	T	3.0	0.2688	2354	0.949	**CHILE_157**	−34.4	−70.8	T	9.0	0.091	797	0.905
0.940	**CHILE_115**	−34.2	−71.4	F	2.7	0.2607	2282	1.004	**CHILE_158**	−27.3	−70.4	T	9.0	0.2331	2041	0.907
0.805	**CHILE_116**	−27.8	−70.1	T	9.0	0.2527	2207	0.926	**CHILE_159**	−27.3	−70.4	T	9.0	0.2308	2021	0.904
0.901	**CHILE_117**	−34.4	−71.7	T	9.0	0.1827	1418	0.982	**CHILE_160**	−33.3	−70.9	T	3.0	0.2334	2044	0.821
0.928	**CHILE_118**	−34.4	−71.6	T	2.9	0.0895	784	0.818	**CHILE_161**	−35.1	−71.6	T	3.0	0.2175	1832	0.947
0.901	**CHILE_119**	−32.8	−70.7	T	3.0	0.2197	1922	0.947	**CHILE_162**	−35.9	−71.8	T	3.0	0.0426	373	0.800
0.825	**CHILE_120**	−32.3	−71.1	T	3.0	0.1303	1141	0.876	**CHILE_163**	−34.3	−71.6	F	3.0	0.1011	807	0.866
0.556	**CHILE_121**	−34.0	−70.7	T	9.0	0.2621	2294	0.908	**CHILE_164**	−32.7	−70.9	F	1.1	0.1879	1646	0.766
0.903	**CHILE_122**	−32.1	−71.2	T	2.0	0.1157	1011	0.900	**CHILE_165**	−30.0	−70.8	F	2.9	0.2116	1853	0.846
0.846	**CHILE_123**	−32.8	−71.1	T	3.0	0.2306	2020	0.946	**CHILE_166**	−33.5	−70.5	F	0.2	0.1108	860	0.626
0.545	**CHILE_124**	−33.3	−71.4	T	9.0	0.2258	1905	0.903	**CHILE_167**	−32.8	−71.0	T	3.0	0.1068	935	0.897
0.757	**CHILE_125**	−33.1	−70.8	T	9.0	0.2542	2225	0.843	**CHILE_168**	−23.6	−70.2	T	52.8	0.3336	2919	0.890
0.880	**CHILE_126**	−31.2	−71.0	F	2.0	0.2475	2168	0.920	Lat: Latitude [°]		Pnet: Net Power [MWp]					
0.565	**CHILE_127**	−31.2	−71.0	F	2.0	0.2502	2192	0.929	Lat: Longitude [°]		UCFn: Net Unit Capacity Factor					
0.796	**CHILE_128**	−26.3	−69.9	T	68.0	0.3129	2741	0.828	MC: Mounting Structure		Yfn: Net Final Yield [kWh/kWp]					
									T: Tracking		PRn: Net Performance Ratio					
									F: Fixed							
0.996	**CHILE_129**	−25.5	−70.2	F	69.4	0.3393	2970	0.933								

Appendix C. Results of comparison between modelled and measured irradiance data

Table C1

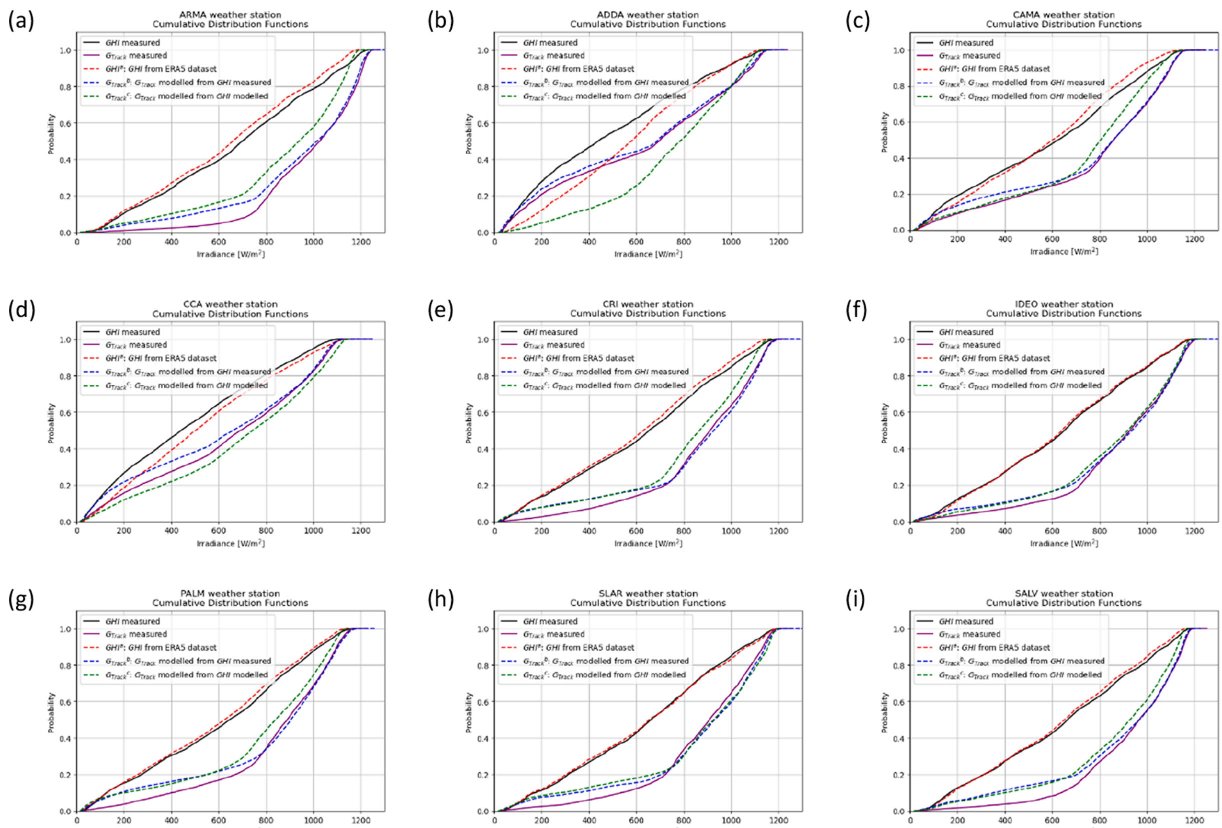

Table C1
Comparison of modelled and measured solar irradiance.

Station	Indicator	GHI^{a}	$G_{Track}{}^{b}$	$G_{Track}{}^{c}$
ADDA	R^2	0.86	0.99	0.78
	MBE [W/m^2]	40.55	−9.12	54.82
	RMSE [W/m^2]	133.46	41.67	200.80
ARMA	R^2	0.99	0.97	0.95
	MBE [W/m^2]	−15.54	−21.71	−50.96
	RMSE [W/m^2]	39.06	91.40	129.07
CAMA	R^2	0.95	0.98	0.89
	MBE [W/m^2]	−6.62	−12.79	−21.96
	RMSE [W/m^2]	80.74	58.39	148.53
CCA	R^2	0.95	0.98	0.92
	MBE [W/m^2]	23.09	−17.77	22.04
	RMSE [W/m^2]	75.91	62.95	118.05
CRI	R^2	0.99	0.97	0.95
	MBE [W/m^2]	−10.79	−9.84	−29.82
	RMSE [W/m^2]	42.32	75.66	103.56
IDEO	R^2	0.99	0.98	0.97
	MBE [W/m^2]	−1.39	−10.00	−13.12
	RMSE [W/m^2]	35.65	61.89	82.88
PALM	R^2	0.98	0.97	0.94

(continued on next page)

Table C1 (*continued*)

Station	Indicator	GHI^a	$G_{Track}{}^b$	$G_{Track}{}^c$
	MBE [W/m^2]	−8.16	−15.11	−30.45
	RMSE [W/m^2]	51.33	85.20	111.69
SALV	R^2	0.99	0.97	0.96
	MBE [W/m^2]	−5.48	−22.70	−30.91
	RMSE [W/m^2]	32.89	91.83	106.99
SLAR	R^2	0.97	0.98	0.94
	MBE [W/m^2]	−0.62	−4.79	−8.12
	RMSE [W/m^2]	62.37	68.17	105.41
SPA	R^2	0.98	0.97	0.94
	MBE [W/m^2]	3.28	−11.17	−8.19
	RMSE [W/m^2]	55.75	80.93	112.77
PANG	R^2	0.94	0.98	0.88
	MBE [W/m^2]	30.96	−13.71	43.32
	RMSE [W/m^2]	91.68	57.88	156.04

[a] *GHI*: *GHI* from ERA5 dataset.
[b] G_{Track}: G_{Track} modelled from *GHI* measured.
[c] G_{Track}: G_{Track} modelled from *GHI* modelled.

Appendix D. Supplementary material

Supplementary data to this article can be found online at https://doi.org/10.1016/j.solener.2021.07.007.

References

Afanasyeva, S., Bogdanov, D., Breyer, C., 2018. Relevance of PV with single-axis tracking for energy scenarios. Sol. Energy 173, 173–191. https://doi.org/10.1016/j.solener.2018.07.029.

Agostini, C.A., Nasirov, S., Silva, C., 2016. Solar PV Planning Toward Sustainable Development in Chile: Challenges and Recommendations. J. Environ. Develop. 25 (1), 25–46. https://doi.org/10.1177/1070496515606175.

Antuko, 2020. Chile: Vertimiento a su más alto nivel desde casi 2 años. [Online]. Available: https://antuko.com/chile-vertimiento-a-su-mas-alto-nivel-desde-casi-2-anos/#_ftnref1 (accessed: Jun. 06, 2021).

Armijo, J., Philibert, C., 2020. Flexible production of green hydrogen and ammonia from variable solar and wind energy: Case study of Chile and Argentina. Int. J. Hydrogen Energy 45 (3), 1541–1558. https://doi.org/10.1016/j.ijhydene.2019.11.028.

Ascencio-Vásquez, J., Topič, M., 2017. An overall data analysis methodology for PV energy systems. In: Conference proceedings 2017. https://repozitorij.uni-lj.si/IzpisGradiva.php?id=113245 (accessed Nov. 11, 2020).

Ascencio-Vásquez, J., Brecl, K., Topič, M., 2019. Methodology of Köppen-Geiger-Photovoltaic climate classification and implications to worldwide mapping of PV system performance. Sol. Energy 191, 672–685. https://doi.org/10.1016/j.solener.2019.08.072.

Ascencio-Vásquez, J., Bevc, J., Reba, K., Brecl, K., Jankovec, M., Topič, M., 2020. Advanced PV Performance Modelling Based on Different Levels of Irradiance Data Accuracy. Energies 13 (9), 2166. https://doi.org/10.3390/en13092166.

Ascencio-Vásquez, J., Brecl, K., Topič, M., 2020. Geographical approach for weather risk identification and PV performance assessment. Presented at the Session Reference: 5DO.2.1, Abstract No. [342].

ATAMOSTEC, 2020. The ATAMO bifacial module developed in Chile, specially adapted to high radiation and desert conditions, sees first success. http://www.atamostec.cl/en/the-atamo-bifacial-module-developed-in-chile-specially-adapted-to-high-radiation-and-desert-conditions-sees-first-success/ (accessed May 17, 2020).

BloomberfNEF, 2019. Chile Power System Outlook. [Online]. Available: https://data.bloomberglp.com/professional/sites/24/Flexibility-Solutions-for-High-Renewable-Energy-Systems-Chile-Outlook.pdf (accessed: May 05, 2020).

Boait, P., Advani, V., Gammon, R., 2015. Estimation of demand diversity and daily demand profile for off-grid electrification in developing countries. Energy Sustain. Develop. 29, 135–141. https://doi.org/10.1016/j.esd.2015.10.009.

Bogdanov, D., et al., 2019. Radical transformation pathway towards sustainable electricity via evolutionary steps. Nat. Commun. 10 (1), 1077. https://doi.org/10.1038/s41467-019-08855-1.

Bolinger, M., Gorman, W., Millstein, D., Jordan, D., 2020. System-level performance and degradation of 21 GWDC of utility-scale PV plants in the United States. J. Renew. Sustain. Energy 12 (4), 043501. https://doi.org/10.1063/5.0004710.

Bustos, C., Watts, D., Olivares, D., 2019. The evolution over time of Distributed Energy Resource's penetration: A robust framework to assess the future impact of prosumage under different tariff designs. Appl. Energy 256, 113903. https://doi.org/10.1016/j.apenergy.2019.113903.

Camargo, L.R., Schmidt, J., 2020. Simulation of long-term time series of solar photovoltaic power: is the ERA5-land reanalysis the next big step? arXiv: 2003.04131. [Online]. Available: arXiv:2003.04131.

Cebecauer, T., Suri, M., 2015. Typical Meteorological Year Data: SolarGIS Approach. Energy Procedia 69, 1958–1969. https://doi.org/10.1016/j.egypro.2015.03.195.

Comision Nacional de Energia (CNE) Chile, 2020. Reporte Mensual Sector Energetico - Marzo 2020, vol. 43.

Comision Nacional de Energia (CNE) Chile, 2020. "Energia Abierta." http://energiaabierta.cl/ (accessed Mar. 04, 2020).

Coordinador Electrico Nacional, 2021. Propuesta de Expansión de la Transmisión 2021. [Online]. Available: https://www.cne.cl/wp-content/uploads/2021/01/Informe-Propuesta-de-Expansi%C3%B3n-2021.pdf (accessed: Jun. 06, 2021).

Copernicus Climate Change Service (C3S), 2017. ERA5: Fifth generation of ECMWF atmospheric reanalyses of the global climate. Copernicus Climate Change Service Climate Data Store (CDS). Copernicus Climate Change Service (C3S). [Online]. Available: https://cds.climate.copernicus.eu/cdsapp#!/home (accessed: Aug. 20, 2019).

Cordero, R.R., et al., 2018. Effects of soiling on photovoltaic (PV) modules in the Atacama Desert. Sci. Rep. 8 (1), 13943. https://doi.org/10.1038/s41598-018-32291-8.

Csoknyai, T., Legardeur, J., Akle, A.A., Horváth, M., 2019. Analysis of energy consumption profiles in residential buildings and impact assessment of a serious game on occupants' behavior. Energy Build. 196, 1–20. https://doi.org/10.1016/j.enbuild.2019.05.009.

Deline, C., et al., 2020. PV Fleet Performance Data Initiative Program and Methodology. In: 2020 47th IEEE Photovoltaic Specialists Conference (PVSC), pp. 1363–1367. https://doi.org/10.1109/PVSC45281.2020.9300583.

Deline, C. et al., 2021. PV Fleet Performance Data Initiative:Performance Index–Based Analysis. National Renewable Energy Laboratory, Golden, CO, NREL/TP-5K00-78720. [Online]. Available: https://www.nrel.gov/docs/fy21osti/78720.pdf.

Encare, Energia 360, 2017. Estudio Benchmarking de Plantas Solares Fotovoltaicas en Chile.

Erbs, D.G., Klein, S.A., Duffie, J.A., 1982. Estimation of the diffuse radiation fraction for hourly, daily and monthly-average global radiation. Sol. Energy 28 (4), 293–302. https://doi.org/10.1016/0038-092X(82)90302-4.

Gaete-Morales, C., Gallego-Schmid, A., Stamford, L., Azapagic, A., 2019. A novel framework for development and optimisation of future electricity scenarios with high penetration of renewables and storage. Appl. Energy 250, 1657–1672. https://doi.org/10.1016/j.apenergy.2019.05.006.

Girard, A., Roberts, C., Simon, F., Ordoñez, J., 2019. Solar electricity production and taxi electrical vehicle conversion in Chile. J. Cleaner Prod. 210, 1261–1269. https://doi.org/10.1016/j.jclepro.2018.11.092.

Haas, J., et al., 2018a. Sunset or sunrise? Understanding the barriers and options for the massive deployment of solar technologies in Chile. Energy Policy 112, 399–414. https://doi.org/10.1016/j.enpol.2017.10.001.

Haas, J., et al., 2020. Copper mining: 100% solar electricity by 2030? Appl. Energy 262, 114506. https://doi.org/10.1016/j.apenergy.2020.114506.

Haas, J., Cebulla, F., Nowak, W., Rahmann, C., Palma-Behnke, R., 2018b. A multi-service approach for planning the optimal mix of energy storage technologies in a fully-renewable power supply. Energy Convers. Manage. 178, 355–368. https://doi.org/10.1016/j.enconman.2018.09.087.

Haas, J., Nowak, W., Palma-Behnke, R., 2019. Multi-objective planning of energy storage technologies for a fully renewable system: Implications for the main stakeholders in Chile. Energy Policy 126, 494–506. https://doi.org/10.1016/j.enpol.2018.11.034.

Haegel, N.M., et al., 2019. Terawatt-scale photovoltaics: Transform global energy. Science 364 (6443), 836–838. https://doi.org/10.1126/science.aaw1845.

Hay, J.E., Davies, J.A., 1980. Calculation of the Solar Radiation Incident on an Inclined Surface, Toronto, Canada.
Hirschmann, R.J., 1973. Records on solar radiation in Chile. Sol. Energy 14 (2), 129–138. https://doi.org/10.1016/0038-092X(73)90029-7.
Huld, T., Paietta, E., Zangheri, P., Pinedo Pascua, I., 2018. Assembling Typical Meteorological Year Data Sets for Building Energy Performance Using Reanalysis and Satellite-Based Data. Atmosphere 9 (2), 53. https://doi.org/10.3390/atmos9020053.
IEA PVPS Task 1, 2020. Snapshot of Global PV Markets - 2020.
Informe de Auditoría DO PES Quilapilún, 2020. [Online]. Available: https://sic.coordinador.cl/wp-content/uploads/2016/01/Informe-de-Auditor%C3%ADa-DO-Quilapil%C3%BAn-Final.pdf (accessed: Jun. 05, 2020).
International Electrotechnical Comission, IEC 61724-1 ED2: Photovoltaic system performance – Part 1: Monitoring.
International Organization for Standardization, 2018. ISO 3166 — Codes for the representation of names of countries and their subdivisions. [Online]. Available: https://www.iso.org/obp/ui/#iso:code:3166:CL (accessed: May 05, 2020).
Jacobson, M.Z., Delucchi, M.A., Cameron, M.A., Mathiesen, B.V., 2018. Matching demand with supply at low cost in 139 countries among 20 world regions with 100% intermittent wind, water, and sunlight (WWS) for all purposes. Renew. Energy 123, 236–248. https://doi.org/10.1016/j.renene.2018.02.009.
Jacobson, M.Z., Jadhav, V., 2018. World estimates of PV optimal tilt angles and ratios of sunlight incident upon tilted and tracked PV panels relative to horizontal panels. Sol. Energy 169, 55–66. https://doi.org/10.1016/j.solener.2018.04.030.
Jäger-Waldau, Arnulf, 2021. Snapshot of photovoltaics - March 2021. EPJ Photovolt. 12, 2. https://doi.org/10.1051/epjpv/2021002.
Jäger-Waldau, A., 2019. European Commission, and Joint Research Centre. Pv status report 2019. [Online]. Available: https://op.europa.eu/publication/manifestation_identifier/PUB_KJNA29938ENN (accessed: May 06, 2020).
Jiang, H., Yang, Y., Bai, Y., Wang, H., 2020. Evaluation of the Total, Direct, and Diffuse Solar Radiations From the ERA5 Reanalysis Data in China. IEEE Geosci. Remote Sens. Lett. 17 (1), 47–51. https://doi.org/10.1109/LGRS.2019.2916410.
Kumar, M., Kumar, A., 2017. Performance assessment and degradation analysis of solar photovoltaic technologies: A review. Renew. Sustain. Energy Rev. 78 (C), 554–587. https://doi.org/10.1016/j.rser.2017.04.08.
Kurtz, S. et al., 2013. Analysis of Photovoltaic System Energy Performance Evaluation Method. doi: 10.2172/1111193.
Leloux, J., Taylor, J., Moretón, R., Narvarte, L., Trebosc, D., Desportes, A., 2015. Monitoring 30,000 PV systems in Europe: Performance, Faults, and State of the Art, vol. 5AO.8.1, pp. 1574–1582. doi: 10.4229/EUPVSEC20152015-5AO.8.1.
Leloux, J., Narvarte, L., Trebosc, D., 2012. Review of the performance of residential PV systems in France. Renew. Sustain. Energy Rev. 16 (2), 1369–1376. https://doi.org/10.1016/j.rser.2011.10.018.
Leloux, J., Narvarte, L., Trebosc, D., 2012. Review of the performance of residential PV systems in Belgium. Renew. Sustain. Energy Rev. 16 (1), 178–184. https://doi.org/10.1016/j.rser.2011.07.145.
Leloux, J., Narvarte, L., Desportes, A., Trebosc, D., 2020. Performance to Peers (P2P): A benchmark approach to fault detections applied to photovoltaic system fleets. Sol. Energy 202, 522–539. https://doi.org/10.1016/j.solener.2020.03.015.
Liang, T.S., et al., 2019. A review of crystalline silicon bifacial photovoltaic performance characterisation and simulation. Energy Environ. Sci. 12 (1), 116–148. https://doi.org/10.1039/C8EE02184H.
Lindig, S., et al., 2021a. International collaboration framework for the calculation of performance loss rates: Data quality, benchmarks, and trends (towards a uniform methodology). Prog. Photovoltaics Res. Appl. 29 (6), 573–602. https://doi.org/10.1002/pip.3397.
Lindig, S., Ascencio-Vasquez, J., Leloux, J., Moser, D., Reinders, A., 2021b. Performance analysis and degradation of a large fleet of PV systems. IEEE J. Photovoltaics 2021. https://doi.org/10.1109/JPHOTOV.2021.3093049.
Lorenzo, E., Narvarte, L., Muñoz, J., 2011. Tracking and back-tracking. Prog. Photovolt: Res. Appl. 19 (6), 747–753. https://doi.org/10.1002/pip.1085.
Mena, R., Escobar, R., Lorca, Á., Negrete-Pincetic, M., Olivares, D., 2019. The impact of concentrated solar power in electric power systems: A Chilean case study. Appl. Energy 235, 258–283. https://doi.org/10.1016/j.apenergy.2018.10.088.
Ministerio de Energia, Gobierno de Chile, 2014. Energias Renovables en Chile: el potencial eolico, solar e hidroelectrico de Arica a Chiloe. [Online]. Available: http://www.minenergia.cl/archivos_bajar/Estudios/Potencial_ER_en_Chile_AC.pdf (accessed: Apr. 21, 2020).
Moreira-Munoz, A., 2011. Plant Geography of Chile. Springer Netherlands. [Online]. Available: https://books.google.si/books?id=hmH11ybGdQEC.
National Institute of Standards and Technology. NIST/SEMATECH e-Handbook of Statistical Methods. Chapter 1.3.5.11. Measures of Skewness and Kurtosis. doi: https://doi.org/10.18434/M32189.
Nobre, A.M., Karthik, S., Liew, W.Y., Baker, R., Malhotra, R., Khor, A., 2019. Performance Evaluation of a Fleet of Photovoltaic Systems Across India and Southeast Asia. In: 2019 IEEE 46th Photovoltaic Specialists Conference (PVSC), pp. 1372–1376. https://doi.org/10.1109/PVSC40753.2019.8981226.
Osorio Aravena, J.C., Aghahosseini, A., Bogdanov, D., Caldera, U., Muñoz-Cerón, E., Breyer, C., 2020. The role of solar PV, wind energy, and storage technologies in the transition toward a fully sustainable energy system in Chile by 2050 across power, heat, transport and desalination sectors. Int. J. Sustain Energy Plan Manage 77–94. https://doi.org/10.5278/IJSEPM.3385.
Palma Behnke, R. et al., 2019. Chilean NDC Mitigation Proposal: Methodological Approach and Supporting Ambition. Mitigation and Energy Working Group Report, Santiago.
Prina, M.G., Manzolini, G., Moser, D., Vaccaro, R., Sparber, W., 2020. Multi-Objective Optimization Model EPLANopt for Energy Transition Analysis and Comparison with Climate-Change Scenarios. Energies 13 (12). https://doi.org/10.3390/en13123255.
PV Tech.org, 2016. Curtailment of solar power in northern Chile 'no surprise' to developers. https://www.pv-tech.org/news/curtailment-of-solar-power-in-northern-chile-no-surprise-to-developers (accessed May 05, 2020).
Ramirez Camargo, L., Valdes, J., Masip Macia, Y., Dorner, W., 2019. Assessment of on-site steady electricity generation from hybrid renewable energy systems in Chile. Appl. Energy 250, 1548–1558. https://doi.org/10.1016/j.apenergy.2019.05.005.
Reinders, A., et al., 2018. Introducing 'PEARL-PV': Performance and Reliability of Photovoltaic Systems: Evaluations of Large-Scale Monitoring Data. In: 2018 IEEE 7th World Conference on Photovoltaic Energy Conversion (WCPEC) (A Joint Conference of 45th IEEE PVSC, 28th PVSEC 34th EU PVSEC), pp. 0762–0766. https://doi.org/10.1109/PVSC.2018.8547966.
Revista Electricidad, 2020. Vertimiento de generación ERNC de noviembre fue el más alto en años: 59,7 GWh. [Online]. Available: https://www.revistaei.cl/2020/12/17/vertimiento-de-generacion-ernc-de-noviembre-fue-el-mas-alto-en-anos-597-gwh/ (accessed: Jun. 06, 2020).
Rondanelli, R., Molina, A., Falvey, M., 2015. The Atacama Surface Solar Maximum. Bull. Amer. Meteor. Soc. 96 (3), 405–418. https://doi.org/10.1175/BAMS-D-13-00175.1.
Solar Power Europe, 2020. Global Market Outlook For Solar Power/2019–2023.
Stefano, A.D., Leotta, G., Bizzarri, F., 2017. La Silla PV plant as utility-scale side-by-side test for innovative modules technologies, p. 5.
Stein, J.S., Holmgren, W.F., Forbess, J., Hansen, C.W., 2016. PVLIB: Open source photovoltaic performance modeling functions for Matlab and Python. In: 2016 IEEE 43rd Photovoltaic Specialists Conference (PVSC), Portland, OR, USA, Jun. 2016, pp. 3425–3430. https://doi.org/10.1109/PVSC.2016.7750303.
Tjengdrawira, Caroline, Moser, David, Jahn, Ulrike, Armansperg, Matthias V., Theologitis, Ioannis-Thomas, Heisz, Máté, 2017. PV Investment Technical Risk Management. Best Practice Guidelines for Risk Identification, Assessment and Mitigation. Deliverable D5.8. Solar Bankability. [Online]. Available: http://www.solarbankability.eu (accessed: Jul. 23, 2020).
Urrejola, E., et al., 2016. Effect of soiling and sunlight exposure on the performance ratio of photovoltaic technologies in Santiago, Chile. Energy Convers. Manage. 114, 338–347. https://doi.org/10.1016/j.enconman.2016.02.016.
Valdes, J., Macia, Y.M., Dorner, W., Camargo, L.R., 2021. Unsupervised grouping of industrial electricity demand profiles: Synthetic profiles for demand-side management applications. Energy 215, 118962. https://doi.org/10.1016/j.energy.2020.118962.
Vartiainen, E., Masson, G., Breyer, C., Moser, D., Román Medina, E., 2019. Impact of weighted average cost of capital, capital expenditure, and other parameters on future utility-scale PV levelised cost of electricity. Prog. Photovolt. Res. Appl. 1–15. https://doi.org/10.1002/pip.3189.
Woyte, A., Richter, M., Moser, D., Mau, S., Reich, N., Jahn, U., 1013. Monitoring of photovoltaic systems: good practices and systematic analysis, vol. 5CO.6.1, pp. 3686–3694. doi: 10.4229/28thEUPVSEC2013-5CO.6.1.
Zurita, A., et al., 2018. State of the art and future prospects for solar PV development in Chile. Renew. Sustain. Energy Rev. 92, 701–727. https://doi.org/10.1016/j.rser.2018.04.096.